Atmos. Meas. Tech. Discuss., doi:10.5194/amt-2016-321, 2016
Manuscript under review for journal Atmos. Meas. Tech.
Published: 12 October 2016

Atmospheric Measurement Techniques
Discussions
Open Access

Assessing the accuracy of microwave radiometers and radio acoustic sounding systems for wind energy applications

Laura Bianco[1,2], Katja Friedrich[3], James Wilczak[2], Duane Hazen[1,2], Daniel Wolfe[1,2], Ruben Delgado[4], Steve Oncley[5], and Julie K. Lundquist[3,6]

[1] Cooperative Institute for Research in Environmental Sciences (CIRES), Boulder, CO, USA

[2] National Oceanic and Atmospheric Administration/Earth Systems Research Laboratory/Physical Science division, Boulder, CO, USA

[3] Department of Atmospheric and Oceanic Sciences, University of Colorado, Boulder, CO, USA

[4] University of Maryland Baltimore County, Baltimore, MA, USA

[5] National Center for Atmospheric Research, Boulder, CO, USA

[6] National Renewable Energy Laboratory, Golden, CO, USA

Correspondence to: Laura Bianco (laura.bianco@noaa.gov)

Atmos. Meas. Tech. Discuss., doi:10.5194/amt-2016-321, 2016
Manuscript under review for journal Atmos. Meas. Tech.
Published: 12 October 2016

Atmospheric Measurement Techniques Discussions

Abstract. To assess current remote-sensing capabilities for wind energy applications, a remote-sensing system evaluation study, called XPIA (eXperimental Planetary boundary layer Instrument Assessment), was held in the spring of 2015 at NOAA's Boulder Atmospheric Observatory (BAO) facility. Several remote-sensing platforms were evaluated to determine their suitability for the verification and validation processes used to test the accuracy of numerical weather prediction models.

The evaluation of these platforms was performed with respect to well-defined reference systems: the BAO's 300-m tower equipped at 6 levels (50, 100, 150, 200, 250, and 300m) with 12 sonic anemometers and 6 temperature and relative humidity sensors; and approximately 60 radiosonde launches.

In this study we first employ these reference measurements to validate temperature profiles retrieved by two co-located microwave radiometers, as well as virtual temperature measured by co-located wind profiling radars equipped with radio acoustic sounding systems. Results indicate a mean absolute error in the temperature retrieved by the microwave radiometers below 1.5 °C in the lowest 5 km of the atmosphere, and a mean absolute error in the virtual temperature measured by the radio acoustic sounding systems below 0.8 °C in the layer of the atmosphere covered by these measurements (up to approximately 1.6 – 2 km). We also investigated the benefit of the vertical velocity applied to the speed of sound before computing the virtual temperature by the radio acoustic sounding systems. We find that using this correction frequently increases the RASS error, and that it should not be routinely applied to all data.

Water vapor density profiles measured by the MWRs were also compared with similar measurements from the soundings, showing the capability of MWRs to follow the vertical profile measured by the sounding, and finding a mean absolute error below 0.5 g m^{-3} in the lowest 5 km

Atmos. Meas. Tech. Discuss., doi:10.5194/amt-2016-321, 2016
Manuscript under review for journal Atmos. Meas. Tech.
Published: 12 October 2016

Atmospheric Measurement Techniques Discussions
Open Access

of the atmosphere. However, the relative humidity profiles measured by the microwave radiometer lack the high-resolution details available from radiosonde profiles. An encouraging and significant finding of this study was that the coefficient of determination between the lapse rate measured by the microwave radiometer and the tower measurements over the tower levels between 50 and 300 m ranged from 0.76 to 0.91, proving that these remote-sensing instruments can provide accurate information on atmospheric stability conditions in the lower boundary layer.

1. Introduction

While the increasing deployment of wind turbines increases society's reliance on renewably-generated electricity, the need for accurate forecasts of that power production also is growing (Marquis et al., 2011). Improving wind forecasts at hub height remains the top priority, but challenges derive from the complexity of physical processes occurring at a wide range of spatial and temporal scales. Fundamental to understanding and accurately forecasting these processes is the accurate measurement of the atmospheric parameters such as wind, temperature, and humidity in four-dimensional space. Assessing the capability and accuracy of remote-sensing instruments to capture planetary boundary layer and flow characteristics was one goal of the DOE- and NOAA-sponsored eXperimental Planetary boundary layer Instrumentation Assessment (XPIA; Lundquist et al. 2016) campaign conducted in the spring 2015 at the Boulder Atmospheric Observatory (BAO), located in Erie, Colorado (~20 km east of Boulder and ~30 km north of Denver).

Herein, we address some of the objectives of the XPIA campaign – determining the accuracy of temperature, water vapor density, and humidity profiles from state-of-the-art remote-sensing instruments such as Microwave Radiometers (MWRs) and Wind Profiling Radars (WPRs) equipped with a Radio Acoustic Sounding System (RASS), and assessing the capability of these active and passive remote-sensing instruments to provide accurate information on atmospheric stability conditions in the lower atmospheric boundary layer. These remote-sensing instruments operated side-by-side during XPIA and are compared to *in-situ* observations from instruments mounted on a 300-m meteorological tower and radiosondes.

Several studies have focused on evaluating the accuracy of temperature, water vapor density, and humidity retrieved by MWRs (e.g., Güldner and Spänkuch 2001; Liljegren et al. 2001; Ware et al. 2003; Cimini et al. 2011; Friedrich et al. 2012) and virtual temperature retrieved by WPRs with RASS (May et al., 1989; Moran and Strauch, 1994; Angevine et al., 1998; Görsdorf and Lehmann, 2000). Studies evaluating the accuracy of MWR measurements using radiosonde observations show consistent results with differences of 1 – 2 K in temperature, <0.4 g m^{-3} in water vapor density, and < 20% in humidity for most weather conditions (Güldner and Spänkuch 2001; Liljegren et al. 2001; Ware et al. 2003; Cimini et al. 2011). Similar results were derived from comparisons between MWR and *in-situ* tower observations with differences in temperature ranging from 0.7 – 1.7 K (Friedrich et al. 2012). Studies evaluating the accuracy of RASS measurements using radiosonde and *in-situ* tower observations show root mean square differences of below 1 ^{o}C in virtual temperature (May et al., 1989; Moran and Strauch, 1994; Angevine et al., 1998). Variations in the results were often a function of various factors such as height above ground, season, topography, abrupt changes in the lapse rate, and regional differences in the surrounding vegetation.

The analysis presented here builds on the results of these previous studies, but also focuses on several unique aspects. First, in our study we provide a comprehensive assessment and comparison of the accuracy of active (two different RASS systems operating side-by-side in similar modes) and passive (two identical MWRs operating side-by-side in identical modes) remote sensing instruments operated over the period of the XPIA campaign under various meteorological conditions, including cold stable air masses, downslope wind conditions, convective conditions, and rain and snow conditions. The accuracies of the retrievals for the two MWR systems were compared to each other as well as to several *in-situ* radiosonde soundings and to the tower observations. Virtual temperatures from a 915-MHz WPR with RASS and a 449-MHz WPR with RASS were also analyzed and compared to *in-situ* radiosonde soundings and tower observations. A second important contribution of this study is to specifically investigate and compare the ability of these active and passive remote-sensing instruments to measure lapse rate to be used for wind energy applications. Knowing the atmospheric stability is indubitably important for wind energy applications such as wind turbine operations, as atmospheric turbulence and wind shear are affected by changes in atmospheric stability. Furthermore, as found in Warthon and Lunquist (2012), and Vanderwende and Lundquist (2012), atmospheric stability impacts both turbine power production (stable conditions improve power performance while the opposite is true for strongly unstable conditions) and wake characteristics (Hansen et al., 2012).

This paper is organized as follows: Section 2 summarizes the experimental design and instrument characteristics; Sections 3 and 4 assesses the accuracy of temperature and lapse rates derived from MWRs and RASSs, respectively; in Section 5 water vapor density and humidity from the MWRs are compared to *in-situ* measurements. Finally, conclusions are presented in Section 6.

2. Experimental design, instruments and methods

2.1 Experimental design

We assess temperature, water vapor density, and relative humidity accuracy from remote-sensing instruments by comparing the observations to *in-situ* observations from radiosondes and instruments mounted on a 300-m meteorological tower. The remote sensing instruments include two identical 35-channel (21 in the 22-30 GHz band, and 14 in the 51-59 GHz band) Radiometrics MWRs, one 915-MHz WPR equipped with RASS, and one 449-MHz WPR also

Atmos. Meas. Tech. Discuss., doi:10.5194/amt-2016-321, 2016
Manuscript under review for journal Atmos. Meas. Tech.
Published: 12 October 2016

equipped with RASS. Figure 1 shows the instruments used in this study. A detailed description of the instruments, methods, and their integration into the XPIA campaign can be found in Lundquist et al. (2016). The MWRs and WPR-RASSs operated side-by-side (~2 m apart) at the visitor center, at about 600 m southwest of the 300-m meteorological tower. Radiosondes were launched from the visitor center in March (38 soundings), while the remaining 23 soundings were launched in April and May from the water tank site 1000 m to the southeast of the visitor center (see Fig. 1 in Lundquist et al. 2016 for details).

2.2. *In-situ* observations: Radiosonde and 300-m meteorological tower

Radiosondes were launched during fair weather conditions at 0800 (1400), 1200 (1800), 1600 (2200), and 2000 (0200) LT (UTC) between 9 – 19 March (38 soundings), 15 and 20 – 22 April (10 soundings), and 1 – 4 May (13 soundings) providing, among others, vertical profiles of temperature, dewpoint temperature, and relative humidity between the surface and > 10 km above ground level (AGL). Fourteen of these soundings were released during stable atmospheric conditions, while the remaining forty seven were launched during unstable conditions.

Two types of sounding systems were used during the campaign: the National Center for Atmospheric Research's Mobile GPS Advanced Upper Air Sounding System (MGAUS) was used in March (with a 1 s temporal resolution, an accuracy of 0.25 ^{o}C on temperature and of 1.5% on relative humidity) for launches from the visitor center, while the Vaisala MW31 DigiCORA Sounding System was used in April and May (with a 2 s temporal resolution, an accuracy of 0. 5 ^{o}C on temperature and of 5% on relative humidity) for launches from the water tank site.

Atmos. Meas. Tech. Discuss., doi:10.5194/amt-2016-321, 2016
Manuscript under review for journal Atmos. Meas. Tech.
Published: 12 October 2016

The 300-m meteorological tower was equipped with temperature and relative humidity sensors at six levels (50, 100, 150, 200, 250, and 300 m) operating continuously at a temporal resolution of 1 s. Temperature was measured with an accuracy better than 0.1 K (Horst et al., 2016).

2.3. Microwave radiometers

Two MWRs, one operated by NOAA (referred to as the NOAA MWR hereafter) and one operated by the University of Colorado (CU MWR), ran side-by-side with identical configurations. Prior to the experiment, both MWRs were calibrated using an external liquid nitrogen target and an internal ambient target (Han and Westwater 2000) and thoroughly serviced (sensor cleaning, radome replacement etc.). Both MWRs observed at the zenith and at an elevation angle of 15° above the ground (referred to as 15° elevation scans hereafter). The instruments were aligned in a way that the 15° elevation scans pointed towards the north and south, approximately parallel to the Colorado Front Range. Microwave emissions at the water vapor (22-30 GZ) and oxygen (51-59 GHZ) absorption band together with infrared emission at 9.6-11.5 microns were used to retrieve vertical profiles of temperature (*T*), water vapor density (*WVD*) and relative humidity (*RH*) every 2-3 minutes using historic radiosondes and a regression methods or neural network (Solheim et al. 1998a, 1998b; Ware et al. 2003). The algorithm, based on a radiative transfer model (Rosenkranz 1998), was trained for both MWRs on a 5-year radiosonde climatology from the Denver, Colorado, National Weather Service sounding archive, based on radiosondes launched at the Denver International Airport, 35 km to the southeast of the instrument site. Note that the MWR observes within an inverted cone with a 2°-3° beam width at 51-59 GHz, and 5°-6° beam width at 22-30 GHz (Ware et al. 2003). Instruments were placed next to each other on a trailer ~3 m off the ground and at a distance of ~2 m to avoid

Atmos. Meas. Tech. Discuss., doi:10.5194/amt-2016-321, 2016
Manuscript under review for journal Atmos. Meas. Tech.
Published: 12 October 2016

interference. Although the instruments use a hydrophobic radome and forced airflow over the surface of the radome during rain, these instruments become less accurate in the presence of rain as some water deposits on the radome. It has been observed that retrieved temperature and humidity profiles from the 15° elevation scans provide higher accuracy during precipitation compared to the zenith observations by minimizing the effect of liquid water and ice on the radiometer radome (Xu et al., 2014).

The vertical resolution of the retrieved profiles ranged from 50 m between the surface and 0.5 km AGL; 100 m between 0.5 to 2 km AGL; and 250 m between 2 and 10 km AGL. Both instruments were also equipped with a rain sensor and a surface sensor for observations of temperature, pressure, and relative humidity. These surface observations serve as a boundary condition for the neural network approach. Since the pressure sensor from the NOAA MWR was broken between 5 – 27 April, the inter-comparison for the NOAA radiometer focuses solely on observations collected between 9 March – 4 April and 28 April – 7 May 2015, while the inter-comparison for the CU radiometer includes all dates between 9 March – 7 May 2015.

2.4. WPR-RASSs

Wind profiling radars are primarily used to measure the vertical profile of the horizontal wind vector (Strauch et al., 1984; Ecklund et al., 1988). The remote measurement of virtual temperature in the lower atmosphere is achieved with the associated RASS, co-located with the WPR. Usually a WPR-RASS system is set up to operate in wind mode for a large fraction of each hour and in RASS mode for the remaining small fraction. When the system is in RASS mode, the RASS emits a longitudinal acoustic wave upward in the air that generates a local

Atmos. Meas. Tech. Discuss., doi:10.5194/amt-2016-321, 2016
Manuscript under review for journal Atmos. Meas. Tech.
Published: 12 October 2016

compression and rarefaction of the ambient air. These density variations are tracked by the Doppler radar and the speed of sound is measured. From the measurement of the speed of sound, the virtual temperature (T_v) in the boundary layer can be obtained (North et al., 1973).

The 915-MHz WPR RASS settings were selected to sample the boundary layer from 120 m to 1618 m in the vertical with a 62 m resolution, while the 449-MHz WPR RASS sampled the boundary layer from 217 m to 2001 m with a 105 m resolution.

Several factors can undermine the accuracy in T_v measurements from RASSs. For example, vertical velocity can influence the accuracy of RASS measurements (May et al., 1989; Moran and Strauch, 1994) because the apparent speed of sound measured by the radar is equal to the sum of the true speed of sound and the vertical air velocity. Previous studies (Moran and Strauch, 1994; Angevine and Ecklund, 1994; Görsdorf and Lehmann, 2000) have found conflicting results on the overall accuracy of T_v measurements by RASSs from correcting the speed of sound for the vertical velocity. Görsdorf and Lehmann (2000) found that the vertical velocity correction improves the accuracy of RASS temperature measurements only in situations when the error of the measured vertical velocities is smaller than the magnitude of vertical velocity itself. This situation is more likely to occur under unstable conditions in the boundary layer. In some cases, they found that this correction can decrease the accuracy of RASS, especially in situations with only light horizontal winds and a lower reliability of vertical wind measurements. Our systems provided both corrected and uncorrected vertical velocity, enabling us to investigate the accuracy of RASS measurements of T_v both corrected and uncorrected for vertical air motion.

Atmos. Meas. Tech. Discuss., doi:10.5194/amt-2016-321, 2016
Manuscript under review for journal Atmos. Meas. Tech.
Published: 12 October 2016

Since the volumes sampled by the MWRs and RASSs are substantially larger than those sampled by the soundings or the tower-based measurements, vertical averaging and linear interpolation were used to facilitate comparison. Particularly, when comparing measurements from MWRs and RASSs to sounding observations we averaged the data of the soundings over the heights of the MWRs and RASSs. When comparing measurements from RASSs to the tower observations we linearly interpolated the data of the tower over the heights of the RASSs, while when comparing measurements from the MWRs to the tower observations no spatial interpolation or averaging was applied since MWR derived temperature levels (0, 50, 100, 150, 200, 250, 300 m) were the same height levels as the in situ tower observations.

3. Accuracy of the temperature profiles

3.1. MWRs versus sounding observations

Differences in temperature between the two MWRs were analyzed before comparing to sounding observations. Profiles derived from 15° elevation scans between the surface and 10 km were compared during the time periods when both instruments were functioning (9/3/2015 – 4/4/2015 in Fig. 2a; 28/4/2015 – 7/5/2015 in Fig. 2b). Note that the off-zenith scans towards the north and south were averaged to reduce the impact of any horizontal inhomogeneity of the atmosphere. Although MWRs operated side-by-side with exactly the same configurations (section 2.3), mean absolute error (MAE) between the two systems ranged between 0.7 – 0.9°C (Fig. 2). Note that the lack of data in April was due to a malfunctioning pressure sensor of the NOAA MWR. In general, the CU MWR observed lower temperatures (T) than did the NOAA MWR with the bias between the two instruments [computed as ($T_{\mathrm{CU\ MWR}}$ - $T_{\mathrm{NOAA\ MWR}}$)] ranging between -0.4 – -

0.6°C. Since the coefficient of determination, R^2, value was 1.00 during the inter-comparison period, we consider the two MWRs in good agreement with each other.

For the comparison between MWRs and sounding observations, the data set was divided into three periods in order to account for differences in the sounding systems and their locations, as well as differences in the atmospheric conditions. The three periods of comparison consist of March, with cooler temperatures and partially snow-covered terrain; May, with mainly warm, convective weather; and a transition period in April with a mixture of cool, rainy and warm, sunny weather. Differences in temperatures between the MWRs and soundings are shown for March in Fig. 3, April in Fig. 4, and May in Fig. 5 between the surface and 5 km AGL. Scatter plot comparisons between soundings and the radiometer observations show that MAEs in temperature were slightly larger in March, ranging between 1.3 – 1.5 °C (Fig. 3a-b) compared to April and May, where values ranged between 0.9 – 1.1°C (Figs. 4a, 5a-b). As previously indicated in Fig. 2, the CU MWR underestimated the temperatures compared to the sounding observations with a bias of -0.3 – -0.8°C in March, April and May. The NOAA MWR showed no bias (defined as T_{MWR} - $T_{\mathrm{Radiosonde}}$) in March but overestimated temperatures in May with a bias of 0.4°C.

Temperatures derived from the MWR zenith scans were also compared to the sounding observations as presented in Table 1. Several studies have suggested to use off-zenith observations at 15° to avoid temperature saturation and reduce scatter (Cimini et al., 2011; Friedrich et al., 2012). In the present data set the zenith measurements performed better than the averaged 15° elevation scans in terms of bias for the CU MWR in March, but not for the NOAA MWR. Despite the higher resolution from the 15° elevation scans, values of MAE and R^2 are surprisingly almost identical for the off-zenith and zenith measurements for all three periods.

Slopes are closer to one for the 15° elevation scans. We decided to base the rest of the study on off-zenith averaged observations at 15° elevation angle because 15° elevation scans provide higher accuracy compared to the zenith observations during precipitation (Xu et al., 2014).

MAE in temperature between the MWRs and radiosondes as a function of height, shown in Figs. 3c, 4b, 5c, indicates two different patterns in the cooler March conditions compared to a warmer April and May. In March, MAEs were below 2°C at altitudes below 3.5 km for the CU MWR with a continuous increase up to 2.7°C at 4.5 km AGL (Fig. 3c). The NOAA MWR showed a similar behavior with a slightly lower MAE that the CU MWR. In April and May, however, MAEs were below ~2°C at all levels not showing the increase in MAE that was seen in March above 3.5 km.

Bias in temperature between the MWRs and radiosondes as a function of height (Figs. 3d, 4c, 5d) showed negative bias in a shallow layer near the surface, positive values below ~1 km (~1.5 km) for the CU (NOAA) MWR and mostly negative values above. The negative bias below 250 m is related to the surface inversions often observed at night or early morning (an example if which is shown in Fig. 6a). The details of the inversion were consistently in error with the MWRs too cold at the surface and too warm above a few hundred meters due to the inversion height being displaced too high. Above 1.5 km, for some of the profiles, radiosonde temperatures strongly differed from the MWR observations (an example if which is shown in Fig. 6b), which might be related to strong observed winds aloft (winds larger than 10 m s^{-1} for these circumstances, not shown) that transported the sounding farther away from the MWR encountering different air masses. Despite their coarser resolution, the MWRs were capable of capturing important gradients in the temperature profile – the existence or lack of surface temperature inversions at around few hundred meters AGL and the overall decrease in temperature with height (examples of which are shown in Fig. 6c-d).

To further evaluate how the transition from a stable nighttime to a more convective boundary layer during the day might affect the accuracy of the temperature observation, the CU MWR retrieved temperatures were compared to the radiosonde temperatures at different times of the day (0700 – 1200 LT; 1300 – 1800 LT; 1900 – 2400 LT), as presented in Fig. 7. This figure contains only the CU MWR because the CU and NOAA MWR were in good agreement over the two periods presented in Fig. 2, and the CU MWR has a larger dataset because of the outage of the NOAA MWR in April. No significant differences between these different times of the day were noticed. For this reason, it can be concluded that the MWR was capable of retrieving temperatures with a MAE of around 1.2 – 1.3°C during different atmospheric stability conditions.

In summary below 3.5 km we find consistent behavior of the MWRs among the different months and similar error statistics for different times of the day using MWR data up to 5 km.

3.2 RASS versus sounding observations

Temperature observations from the RASSs were compared to radiosonde observations in the same manner as for the MWRs. As mentioned in section 2.4, we investigate the accuracy of T_v RASS measurements corrected and uncorrected for vertical air motion. Without the vertical velocity correction (uncorrected T_v), no important differences between the three periods of radiosonde launches emerged (figure not shown). Results of the comparison between uncorrected T_v measurements from the 915-MHz and the 449-MHz RASS and all the radiosondes launched in March, April and May are presented in Fig. 8a, b. The MAE for uncorrected T_v observations was 0.7°C with a bias of 0.2 – 0.3°C (defined as T_{RASS} - $T_{Radiosonde}$). The impact of the vertical velocity correction is shown in the profile of MAE (Fig. 8c). For uncorrected T_v (solid lines), MAEs are below 1 °C throughout the entire RASS sampling height. However, for corrected T_v (dashed lines), MAEs are larger than those for the uncorrected T_v, for both the 915-MHz and 449-MHz RASS, with larger values for the 915-MHz RASS. Similar results were also found for vertical profiles of the bias (Fig. 8d), for both RASSs. The bias is around 0.3 °C for the 915-MHz RASS and remains nearly constant with height (solid blue line); the 449-MHz RASS indicates slightly negative biases below 400 m (solid magenta line), increasing to around 0.2°C above. For both RASSs, the use of the vertical velocity correction in the computation of T_v increases the bias substantially (dashed lines), similarly to the impact on the MAE generated by this correction. This dataset included little convective activity, and so using the values of T_v corrected for the vertical velocity from RASS measurements is not beneficial in this study consistent with the results of Görsdorf and Lehmann (2000). Moreover, the correction is more negative on the 915-MHz RASS T_v which is an indication that the vertical velocity measurements are more difficult for this system compared to the 449-MHz RASS.

3.3. MWRs versus *in-situ* tower observations

In the next step of our assessment, hourly-averaged temperatures from the *in-situ* tower observations were compared to temperatures derived by the CU MWR for all dates between 9 March – 7 May (Fig. 9). The data set was not divided in different months since the overall statistics in section 3.1 indicated little variation between the months. The CU MWR is in better agreement with the tower observations, with a MAE of 0.8 °C (Fig. 9a), than it was with the

Atmos. Meas. Tech. Discuss., doi:10.5194/amt-2016-321, 2016
Manuscript under review for journal Atmos. Meas. Tech.
Published: 12 October 2016

Atmospheric Measurement Techniques Discussions

sounding observations (MAE= 1.2 ^{o}C; Fig. 7a). The MWR temperatures show a positive bias of 0.8 ^{o}C compared to the *in-situ* temperature observations. The vertical profile of MAE calculated between the MWR and *in-situ* temperature observations (Fig. 9b, solid line) indicates higher values of ~1 ^{o}C at 150 – 250 m, which is exactly the heights where the MAE between the MWR and the radiosondes showed a local maximum in MAE (Figs. 3c, 4b, 5c). The vertical profile of bias in temperature between MWR and *in-situ* observations (Fig. 9b, dashed line) show that the bias is the main contribution to the error, as the value of the bias and of the MAE are very similar to each other.

While radiosondes were only launched during rain- and snow-free conditions, the comparison with tower observations (Fig. 9) contains measurements during both times with precipitation and without precipitation. A comparison between MWR and *in-situ* temperatures observations from the tower (Fig. 10) shows that the MAE was slightly lower during rainy conditions (0.8 ^{o}C) than during rain-free conditions (0.9 C), but the overall statistics are not particularly compromised. Note that we used the rainfall sensor MWRs are equipped with to divide the dataset between times with and without precipitation.

3.4. RASS versus *in-situ* tower observations

Hourly-averaged temperatures from the *in-situ* tower observations were compared to temperatures derived by the RASSs for all dates between 9 March – 7 May (Fig. 11). Again, the data set was not divided in different months since the overall statistics in section 3.2 indicated little variation between the months. Since RASS T_v profiles provided data at different heights than the tower observations, hourly averaged tower measurements were linearly interpolated/extrapolated to the 915-MHz RASS's lowest four altitudes (120, 182, 245, and 307 m), and over the 449-MHz RASS's lowest two altitudes (217 and 322 m). As for the comparison with the radiosondes presented in section 3.2, the effect of applying the correction for the vertical velocity to the T_v computation by the RASS systems was again investigated.

For the uncorrected T_v, the MAE for the RASSs were similar when using the *in situ* tower observations (Fig. 11a-b) as when using the radiosonde observations (Fig. 8a-b). For bias, both RASSs slightly underestimated virtual temperatures compared to the tower observations, with a bias of -0.1 ^{o}C for the 915-MHz RASS and -0.4 ^{o}C for the 449-MHz RASS. These numbers are within the expected accuracy of RASS measurements (May et al., 1989).

Vertical profiles of uncorrected T_v MAEs and biases calculated between the tower and both the 915-MHz and 449-MHz RASSs (solid blue and magenta lines in Fig. 11c-d) show more accurate results than when using the RASS vertical velocity correction (dashed blue and magenta lines). As previously found in section 3.2, the vertical velocity correction (dashed lines) was not beneficial to neither the 915-MHz nor the 449-MHz RASS.

We note that comparing Figs. 3-5 to Fig. 8, and Fig. 9 to Fig. 11, the RASS has lower error statistics than the MWRs which was also shown in Fig. 15 of Lundquist et al. 2016.

4. Accuracy of the lapse rate

Several studies have suggested that surface temperature inversions might be smoothed by remote-sensing instruments with coarse spatial resolutions (Solheim et al. 1998b; Reehorst 2001). Nevertheless, accurate representation of the lapse rate and consequently of atmospheric stability is essential for wind energy operators to better predict the presence of vertical wind shear (more likely to happen during stable conditions) and turbulence affecting the load on rotors (more likely to happen during unstable conditions). Although it is more appropriate to use lapse rate of potential temperature or virtual potential temperature to provide information on stability conditions (Friedrich et al, 2012), as a first step we want to compare the ability of MWR with that of the RASS at evaluating atmospheric stability conditions in the lower boundary layer. To allow this comparison, we first computed the lapse rate of temperature ($\gamma_T = -dT/dz$) between 50 m and 300 m observed by the CU MWR and compared it with the *in-situ* tower observations including all dates between 9 March – 7 May (Fig. 12a). Statistics indicate that for the lapse rate of temperature measured by the CU MWR and the *in-situ* tower measurements the MAE was about 2.1 ^{o}C km^{-1} with a R^2 of 0.91. The same analysis was performed for the lapse rate of virtual temperature ($\gamma_{T_v} = -dT_v/dz$) computed between the first and fourth level of the 915-MHz RASS measurements (120-307 m) with the *in-situ* tower observations (Fig. 12b), and for the lapse rate of virtual temperature (γ_{T_v}) computed between the first and second level of the 449-MHz RASS measurements (217-322 m) with the *in-situ* tower observations (Fig. 12c). To have a compatible comparison between the ability of the MWR at measuring lapse rate with that of the RASSs we computed the same statistics (MAE, bias, R^2, slope) presented in Fig. 12a, but first interpolating the CU MWR observations over the heights covered by the 915-MHz RASS over the tower measurements (120-307 m), and later interpolating the MWR observations over the heights covered by the 449-MHz RASS over the tower measurements (217-322 m). The first gave a R^2 = 0.89 for the CU MWR and R^2 = 0.81 for the 915-MHz RASS, while the second gave a R^2 = 0.79 for the CU MWR and R^2 = 0.6 for the 449-MHz RASS, resulting in the best R^2 for the MWR. In addition to the lapse rates of temperature (γ_T), we calculated lapse rate of potential temperature from CU MWR measurements, as $\gamma_\theta = -d\theta/dz$ (differences with the lapse rate of virtual potential temperature were practically unnoticeably). The statistics (MAE, bias, R^2, slope) were calculated for γ_θ using different tower levels and the results are presented in Table 2. We note that the agreement between the lapse rate of potential temperature measured by the CU MWR and the *in-situ* tower measurements is best when it is computed between 50 m and 300 m (larger dz), with a coefficient of determination of 0.91. A comparison between the time series of γ_θ (between 50 and 300 m) as computed by the *in-situ* tower measurements and as computed by the CU MWR is presented in Fig. 13 for all dates between 9 March – 7 May. The CU MWR follows the diurnal cycle of $d\theta/dz$ quite well, with the largest differences occurring at the minimum and maximum values.

To better quantify the differences in temperature between the CU MWR and the *in-situ* observations, the data set was finally divided into times when the atmosphere was stable ($d\theta/dz \geq 0$) and unstable ($d\theta/dz < 0$), based on the observations conducted by the CU MWR presented in Fig. 13. Temperatures observed by the CU MWR were compared during stable and unstable conditions to *in-situ* tower observations at six height levels between 50 – 300 m. Smaller MAE's occurred in unstable conditions (MAE = 0.8 ^{o}C; Fig. 14a) compared to stable conditions (MAE = 1.2 ^{o}C; Fig. 14b). Similarly the bias was smaller in unstable conditions compared to stable, and R^2 was larger.

5. Accuracy of the MWR water vapor density and humidity profiles

Differences in water vapor density (*WVD*) and relative humidity (*RH*) between the two MWRs were analyzed before comparing to sounding observations. Profiles derived from averaged 15^o elevation scans between the surface and 10 m AGL were compared during the time periods when both instruments were functioning (9/3/2015 – 4/4/2015 in Fig. 15a-c; 28/4/2015 – 7/5/2015 in

Fig. 15b-d). For the *WVD* comparison, the MAE's for the two systems were 0.1 and 0.2 g m^{-3}, the biases were ~ 0.1 g m^{-3} and R^2 was very close to 1 (Fig. 15a-b). For the *RH* comparison, the MAE's were 4.1 and 4.8%, the biases were 2.1 and 0.9%, while the coefficients of determination were both 0.96 (Fig. 15c-d). The values of bias, R^2, and slope indicated a good agreement between the instruments over the periods during which they were both functioning properly.

Lastly, water vapor density and relative humidity derived from the MWRs between the surface and 5 km AGL are compared to radiosonde observations from March, April, and May (Figs. 16-19 for *WVD*; Figs. 20-23 for *RH*). For *WVD*, in March and April, MAE for both instruments show values equal to 0.3 g m^{-3}, also reported by Cimini et al. 2011, the bias was close to 0 g m^{-3} and the coefficient of determination was 0.92 (Fig. 16a-b and Fig. 17a). Vertical profiles of MAE (Fig. 16c and Fig. 17b) show values of about 0.3 – 0.2 g m^{-3} up to 3 – 3.5 km, with decreasing MAE above 3.5 km. Larger MAEs were observed for *WVD* in May (Fig. 18) compared to March and April. MAE is equal to 0.5 g m^{-3} (Fig. 18a-b) with R^2 values of about 0.92. Vertical profiles of MAE in May indicate larger values below 2.5 km, where *WVD* profiles from the sounding showed more variability, decreasing above. Overall MWRs are able to follow the radiosonde vertical profile of *WVD* as presented in Fig. 19, although some information is missed due to the coarser MWR resolution compared to the sounding observations.

For *RH*, MAE for both instruments show values below 10 % in March (Fig. 20a-b). A relatively large scatter (R^2 of ~0.8) is an indication of large variation in relative humidity. Some of the variability and associated large scatter might be attributed to the sounding encountering different air masses or even clouds at higher altitudes, as indicated by the vertical profiles of MAE. These profiles show that the MAE's are about 5 – 8% below ~1 km, with the MAE continuously increasing with increasing height (Fig. 20c). Larger MAEs were observed in April and May

Atmos. Meas. Tech. Discuss., doi:10.5194/amt-2016-321, 2016
Manuscript under review for journal Atmos. Meas. Tech.
Published: 12 October 2016

Atmospheric Measurement Techniques Discussions

(Figs. 21-22) compared to March (Fig. 20). MAE's range between 11 – 14% with R^2 values of about 0.5 (Fig. 21a and Fig. 22a-b). Vertical profiles of MAE in April and May indicate a similar pattern compared to March. Lower values (5 – 12%) were observed below ~1 km, while larger values occurred around 1 km and between 3 – 4 km. Since the three-dimensional humidity field is highly variable and strongly depends whether or not the instruments (both MWR and sounding) encountered clouds, the large MAE's between 1 – 4 km are most likely due to changes in air mass or the existence of clouds.

High-resolution soundings with vertical resolution of few meters show much more detail compared to the smooth MWR humidity profiles, as seen in Fig. 23. These examples show that while the MWRs are capable of reproducing the general trend compared to sounding observations, differences between the MWR and the sounding can be as high as 20-25%.

6. Conclusions

Data collected during the XPIA campaign in spring 2015 were used to assess the accuracy of temperature, water vapor density, and relative humidity profiles from two MWRs, one 915-MHz WPR-RASS system, and one 449-MHz WPR-RASS system with respect to *in-situ* reference measurements from 61 radiosonde launches and temperature and relative humidity measurements at six different levels from a 300-m co-located tower. Results indicate a mean absolute error in the temperature retrieved by the MWRs below 1.5 ºC for the layer of the atmosphere up to 5 km. However, the details of the inversions were consistently in error, with the MWRs too cold at the surface and too warm above 250 m. Our results revealed that the overall statistics for MWRs temperature measurements were slightly better for unstable conditions than stable, while the overall statistics for MWR temperature measurements were not

Atmos. Meas. Tech. Discuss., doi:10.5194/amt-2016-321, 2016
Manuscript under review for journal Atmos. Meas. Tech.
Published: 12 October 2016

Atmospheric Measurement Techniques Discussions

particularly compromised during rainy conditions, compared to rain-free conditions. In addition we find consistent behavior of the MWRs among the different months and similar error statistics for different times of the day.

For the RASSs we found a mean absolute error in the virtual temperature below 0.8 ºC in the layer of the atmosphere covered by these measurements (up to approximately 1.6 – 2 km) and that using the values of T_v corrected for the vertical velocity can decrease temperature accuracy, and should only be used with caution. For this dataset, the correction for the vertical velocity applied to calculate T_v was not beneficial to the accuracy of RASS measurements of T_v under any weather condition. In general the RASSs have overall lower error statistics than the MWRs for the layer of the atmosphere covered by the RASSs.

We additionally assessed the accuracy of these remote-sensing instruments at measuring atmospheric stability conditions in the lower boundary layer, finding a coefficient of determination between the lapse rate measured by the MWR and the tower measurements over the tower levels between 50 and 300 m ranged from 0.76 to 0.91, with the best value (0.91) found when the lapse rate is computed between 50 m and 300 m (larger dz). These positive results demonstrate that profiling microwave radiometers can be useful for understanding conditions that can lead to strong vertical wind shear or turbulence, which can affect the load on rotors.

We also assessed the accuracy of MWRs at retrieving water vapor density profiles, finding a mean absolute error below 0.5 g m^{-3} for the layer of the atmosphere up to 5 km.

Finally, our study unsurprisingly revealed that relative humidity profiles measured by the MWR lack high resolution details compared to radiosonde measurements with differences between the MWR and the sounding that can be as high as 20-25% and in average, for the layer of the atmosphere up to 5 km, of the order of 8-14%. For this reason, our future research will utilize the unique dataset collected for XPIA to combine the information obtained from WPR potential refractivity profiles and from MWR potential temperature profiles to improve the accuracy of atmospheric humidity profiles (Bianco et al., 2005).

Acknowledgements

The authors wish to acknowledge Alex St. Pé from University of Maryland, Baltimore County, as well as the University of Colorado Boulder students Joseph C.-Y. Lee, Paul Quelet, Clara St. Martin, Brian Vanderwende, Rochelle Worsnop who launched the radiosondes and Mr. Timothy Lim of NCAR for providing them careful training. We are very grateful for the assistance received from Radiometrics Corporation in setting up and comparing the two MWRs. Thank goes to the University of Colorado Boulder students Joshua Aikins and Evan Kalina who set up the CU radiometer. We express appreciation to the National Science Foundation for supporting the CABL deployments (https://www.eol.ucar.edu/field_projects/cabl) of the MGAUS radiosondes and the tower instrumentation. We thank Lefthand Water District for providing access to the Water Tank site. We would like to acknowledge operational, technical, and scientific support provided by NCAR's Earth Observing Laboratory, sponsored by the National Science Foundation, as well as by Timothy Coleman of NOAA/PSD. Partial support for the UMBC deployments was provided by the Maryland Energy Administration. NREL is a national laboratory of the U. S. Department of Energy, Office of Energy Efficiency and Renewable Energy, operated by the Alliance for Sustainable Energy, LLC. Funding for this work was provided by the U. S. Department of Energy, Office of Energy Efficiency and Renewable

Atmos. Meas. Tech. Discuss., doi:10.5194/amt-2016-321, 2016
Manuscript under review for journal Atmos. Meas. Tech.
Published: 12 October 2016

Energy, Wind and Water Power Technologies Office, and by NOAA's Earth System Research Laboratory.

Atmos. Meas. Tech. Discuss., doi:10.5194/amt-2016-321, 2016
Manuscript under review for journal Atmos. Meas. Tech.
Published: 12 October 2016

Atmospheric Measurement Techniques Discussions

References

Angevine, W. M., and W. Ecklund, 1994: Errors in radio acoustic sounding of temperature, *J. Atmos. Oceanic Technol.*, **11**, 837–842.

Angevine, W. M., P.S. Bakwin, K. J. Davis, 1998: Wind profiler and RASS measurements compared with measurements from a 450-m-tall tower, *J. Atmos. Oceanic Technol.*, **15**, 818–825.

Bianco L., D. Cimini, F. S. Marzano, and R. Ware, 2005: Combining microwave radiometer and wind profiler radar measurements for high-resolution atmospheric humidity profiling, *J. Atmos. Ocean. Tech.*, **22**, 949-965.

Cimini, D., E. Campos, R. Ware, S. Albers, G. Giuliani, J. Oreamuno, P. Joe, S. E Koch, S. Cober, and E. Westwater, 2011: Thermodynamic atmospheric profiling during the 2010 Winter Olympics using ground-based microwave radiometry, *IEEE Transactions on Geoscience and Remote Sensing*, **99**, 1–11. doi:10.1109/TGRS.2011.2154337.

Ecklund, W. L., D. A. Carter, B. B. A. Balsley, 1988: UHF wind profiler for the boundary layer: brief description and initial results, *J. Atmos. Oceanic Technol.*, **5**, 432–41.

Friedrich, K., Lundquist, J.K., Aitken, M., Kalina, E.A. and Marshall, R.F., 2012: Stability and turbulence in the atmospheric boundary layer: A comparison of remote sensing and tower observations, *Geophysical Research Letters*, **39(3)**, doi: 10.1029/2011GL050413.

Görsdorf, U., and V. Lehmann, 2000: Enhanced Accuracy of RASS-Measured Temperatures Due to an Improved Range Correction, *J. Atmos. Oceanic Technol.*, **17**, 406–416.

Atmos. Meas. Tech. Discuss., doi:10.5194/amt-2016-321, 2016
Manuscript under review for journal Atmos. Meas. Tech.
Published: 12 October 2016

Atmospheric Measurement Techniques Discussions

Güldner, J., and D. Spänkuch, 2001: Remote sensing of the thermodynamic state of the atmospheric boundary layer by ground-based microwave radiometry, *J. Atmos. Oceanic Technol.*, **18**, 925–933.

Hansen, K. S., R. J. Barthelmie, L. E. Jensen, and A. Sommer, 2012: The impact of turbulence intensity and atmospheric stability on power deficits due to wind turbine wakes at Horns Rev wind farm, *Wind Energy*, **15(1)**, 183-196, doi: 10.1002/we.512.

Han Y, and E. R. Westwater, 2000: Analysis and improvement of tipping calibration for ground-based microwave radiometers, *IEEE Transactions on Geoscience and Remote Sensing*, ***38(3)***, 1260–1276, doi: 10.1109/36.843018.

Horst, T. W., S. R. Semmer, and I. Bogoev, 2016: Evaluation of Mechanically-Aspirated Temperature/Relative Humidity Radiation Shields, *18th Symposium on Meteorological Observation and Instrumentation, AMS Annual Meeting*, New Orleans, LA, 10-15- January, 2015 (https://ams.confex.com/ams/96Annual/webprogram/Paper286839.html).

Liljegren, J., Lesht, B.M., Kato, S. and Clothiaux, E., 2001: Initial evaluation of profiles of temperature, water vapor and cloud liquid water from a new microwave profiling radiometer. In Preprints, 11th Symp. on Meteorological Observations and Instrumentation, Albuquerque, NM, January 2001, Amer. Meteor. Soc (Vol. 8) (available at: http://radiometrics.com/data/uploads/2012/11/MWRP_ARM01.pdf).

Lundquist, J. K., J. M. Wilczak, R. Ashton, L. Bianco, W. A. Brewer, A. Choukulkar, A. Clifton, M. Debnath, R. Delgado, K. Friedrich, S. Gunter, A. Hamidi, G. V. Iungo, A. Kaushik, B. Kosović, P. Langan, A. Lass, E. Lavin, J. C.-Y. Lee, K. L. McCaffrey, R. K. Newsom, D. C. Noone, S. P. Oncley, P. T. Quelet, S. P. Sandberg, J. L. Schroeder, W. J. Shaw, L. Sparling, C.

Atmos. Meas. Tech. Discuss., doi:10.5194/amt-2016-321, 2016
Manuscript under review for journal Atmos. Meas. Tech.
Published: 12 October 2016

Atmospheric Measurement Techniques Discussions
Open Access

St. Martin, A. St. Pe, E. Strobach, K. Tay, B. J. Vanderwende, A. Weickmann, D. Wolfe, and R. Worsnop, 2016: Assessing state-of-the-art capabilities for probing the atmospheric boundary layer: the XPIA field campaign, *Bull. Amer. Meteor. Soc.*, http://dx.doi.org/10.1175/BAMS-D-15-00151.1.

Marquis, M., J. Wilczak, M. Ahlstrom, J. Sharp, A. Stern, J. C. Smith, and S. Calvert, 2011: Forecasting the wind to reach significant penetration levels of wind energy, *Bull. Amer. Meteor. Soc.*, **92**, 1159–1171, doi:10.1175/2011BAMS3033.1.

May P. T., K. P. Moran, and R. G. Strauch, 1989: The Accuracy of RASS Temperature Measurements, *J. Appl. Meteor.*, **28**, 1329–1335.

Moran K. P., and R. G. Strauch, 1994: The Accuracy of RASS Temperature Measurements Corrected for Vertical Air Motion, *J. Atmos. Oceanic Technol.*, **11**, 406–4016.

North, E. M., A. M. Peterson, and H. D. Parry, 1973: RASS, a remote sensing system for measuring low-level temperature profiles, *Bull. Amer. Meteor. Soc.*, **54**, 912–919.

Reehorst, A. L., 2001: Comparison of profiling microwave radiometer, aircraft, and radiosonde measurements from the Alliance Icing Research Study (AIRS). NASA/TM-2001-211101. 12 p (available at http://ntrs.nasa.gov/archive/nasa/casi.ntrs.nasa.gov/20010098322.pdf)

Rosenkranz P. W., 1998: Water vapor microwave continuum absorption: A comparison of measurements and models, *Radio Science*, **33**, 919–928.

Solheim, F., J. Godwin, and R. Ware, 1998a: Passive ground-based remote sensing of atmospheric temperature, water vapor, and cloud liquid water profiles by a frequency synthesized microwave radiometer, *Met. Z.*, **7**, 370–376.

Solheim, F., J. Godwin, E. Westwater, Y. Han, S. Keihm, K. Marsh, and R. Ware, 1998b: Radiometric profiling of temperature, water vapor and cloud liquid water using various inversion methods, *Radio Science*, ***33***, 393–404.

Strauch, R. G., D. A. Merritt, K. P. Moran, K. B. Earnshaw, and D. Van De Kamp, 1984: The Colorado wind-profiling network, *J. Atmos. Oceanic Technol.*, **1**, 37–49.

Vanderwende, B. J., and J. K. Lundquist, 2012: The modification of wind turbine performance by statistically distinct atmospheric regimes, *Environ. Res. Lett.*, **7**, 034035.

Ware, R., Carpenter, R., Güldner, J., Liljegren, J., Nehrkorn, T., Solheim, F. and Vandenberghe, F., 2003: A multichannel radiometric profiler of temperature, humidity, and cloud liquid, *Radio Science*, **38(4)**.

Wharton, S., and J. K. Lundquist, 2012: Atmospheric stability affects wind turbine power collection. *Environ. Res. Lett.*, **7**, 014005, doi:10.1088/1748-11679326/7/1/014005.

Xu, G., R. Ware, W. Zhang, G. Feng, K. Liao, Y. Liu, 2014: Effect of off-zenith observations on reducing the impact of precipitation on ground-based microwave radiometer measurement accuracy, *Atmospheric Research*, **140-141**, 85-94.

Atmos. Meas. Tech. Discuss., doi:10.5194/amt-2016-321, 2016
Manuscript under review for journal Atmos. Meas. Tech.
Published: 12 October 2016

Table 1. Statistical values for the NOAA and CU MWRs vs radiosonde observations of *T* for the three periods of radiosonde launches and for the zenith and at 15º off-zenith angles. Bias and MAE are in (ºC).

	March (38 radiosonde)				April (13 radiosonde)				May (10 radiosonde)			
	Bias	MAE	R^2	slope	Bias	MAE	R^2	slope	Bias	MAE	R^2	slope
CU MWR (zenith) vs radiosonde	-0.3	1.5	0.98	0.91	0.2	1.1	0.99	0.94	0.2	1.1	0.99	0.93
CU MWR (15º elevation) vs radiosonde	-0.8	1.5	0.98	0.93	-0.2	0.9	0.99	0.97	-0.3	1.1	0.98	0.97
NOAA MWR (zenith) vs radiosonde	-0.5	1.4	0.98	1.03	Missing data				-0.1	1	0.99	1.04
NOAA MWR (15º elevation) vs radiosonde	0	1.3	0.98	0.94	Missing data				0.4	1	0.98	0.97

Atmos. Meas. Tech. Discuss., doi:10.5194/amt-2016-321, 2016
Manuscript under review for journal Atmos. Meas. Tech.
Published: 12 October 2016

Atmospheric Measurement Techniques Discussions

Table 2. Statistical values for the CU MWRs vs tower observations of lapse rate ($\gamma_\theta = -d\theta/dz$) for different tower levels. Bias and MAE are in (°C km^{-1}).

Lapse rate ($\gamma_\theta = -d\theta/dz$) Between 50 - 150 m				Lapse rate ($\gamma_\theta = -d\theta/dz$) Between 50 - 200 m				Lapse rate ($\gamma_\theta = -d\theta/dz$) Between 50 - 250 m				Lapse rate ($\gamma_\theta = -d\theta/dz$) Between 50 - 300 m			
Bias	MAE	R^2	slope	Bias	MAE	R^2	slope	Bias	MAE	R^2	slope	Bias	MAE	R^2	slope
0.76	5.7	0.76	0.59	0.52	4.0	0.82	0.70	-0.19	3.0	0.88	0.81	-0.1	2.2	0.91	0.96

Atmos. Meas. Tech. Discuss., doi:10.5194/amt-2016-321, 2016
Manuscript under review for journal Atmos. Meas. Tech.
Published: 12 October 2016

Atmospheric Measurement Techniques Discussions

Figure 1: Instruments used in this study. From the left: 300-m equipped meteorological tower (photo credit: Katie McCaffrey), radiosonde, 2 MWRs, 915-MHz and RASS system (photo credit: Katie McCaffrey), 449-MHz and RASS system (photo credit: Katie McCaffrey).

Atmos. Meas. Tech. Discuss., doi:10.5194/amt-2016-321, 2016
Manuscript under review for journal Atmos. Meas. Tech.
Published: 12 October 2016

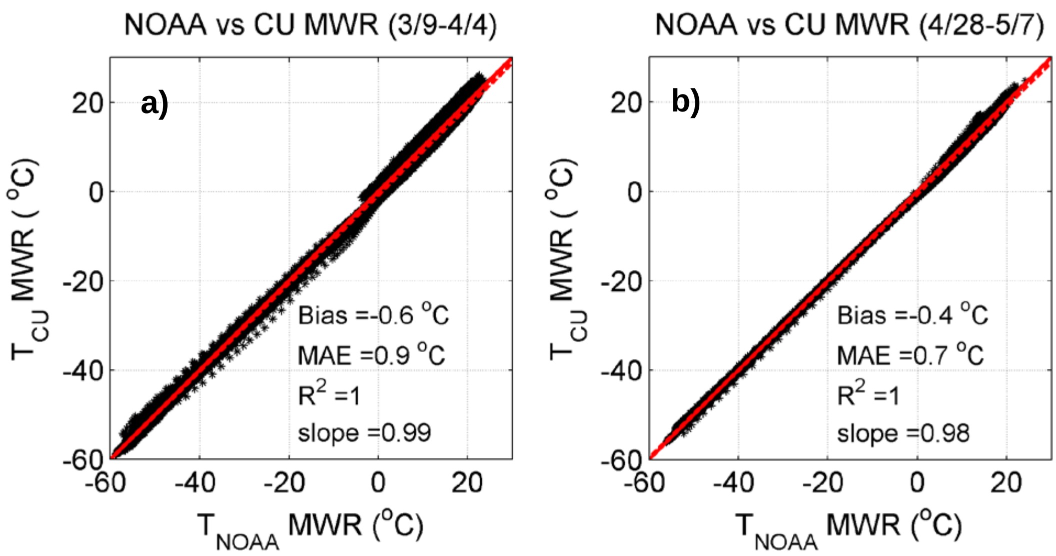

Figure 2: Comparison between temperature observed by CU MWR and NOAA MWR between: a) 9 March – 4 April, and b) 28 April – 7 May, 2015. The missing days in April coincide with the failure of the NOAA MWR surface sensor. A 1-to-1 line is indicated in solid red, and the regression is shown by the dashed red line.

Atmos. Meas. Tech. Discuss., doi:10.5194/amt-2016-321, 2016
Manuscript under review for journal Atmos. Meas. Tech.
Published: 12 October 2016

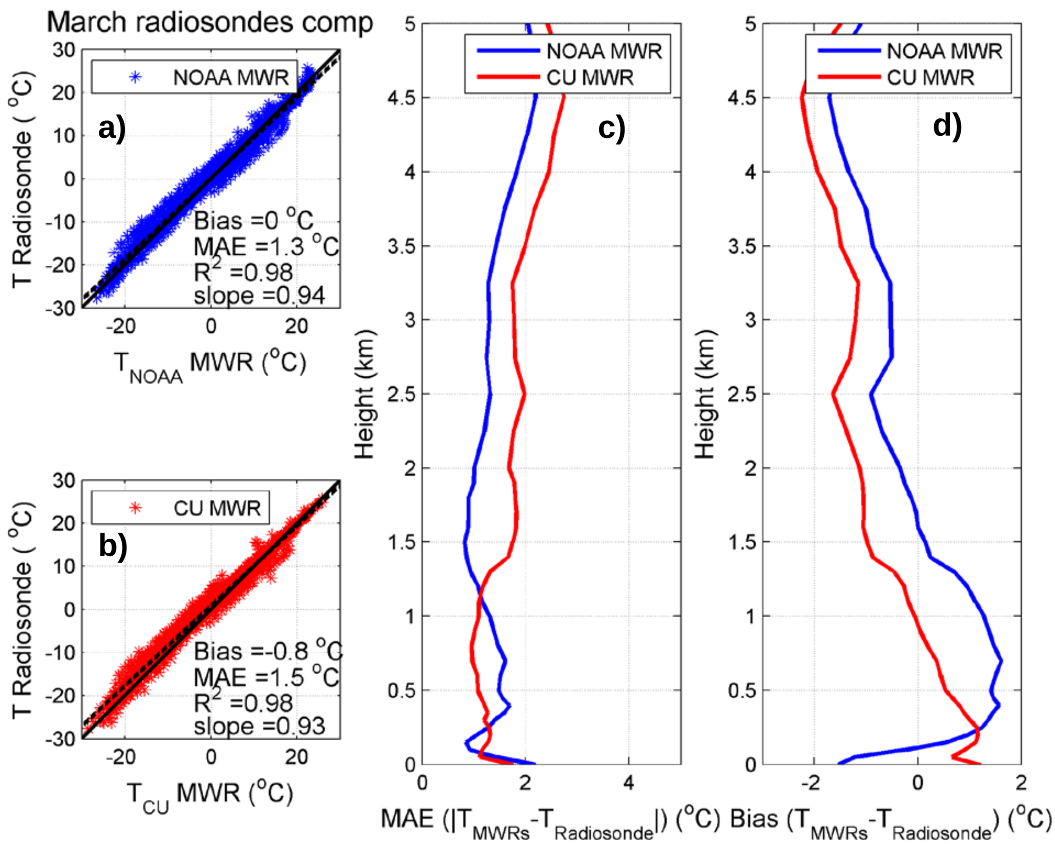

Figure 3: MWRs vs radiosonde comparison of *T* for 9 – 19 March including 38 radiosonde launches: a)-b) One-to-one comparisons between *T* observed by the radiosondes and the a) NOAA and b) CU MWR between the surface and 5 km AGL. One-on-one line is indicated as solid black line and the regression as dashed black line. c)-d) Vertical profiles of MAE and Bias for the same variable for the NOAA MWR (blue line) and CU MWR (red line).

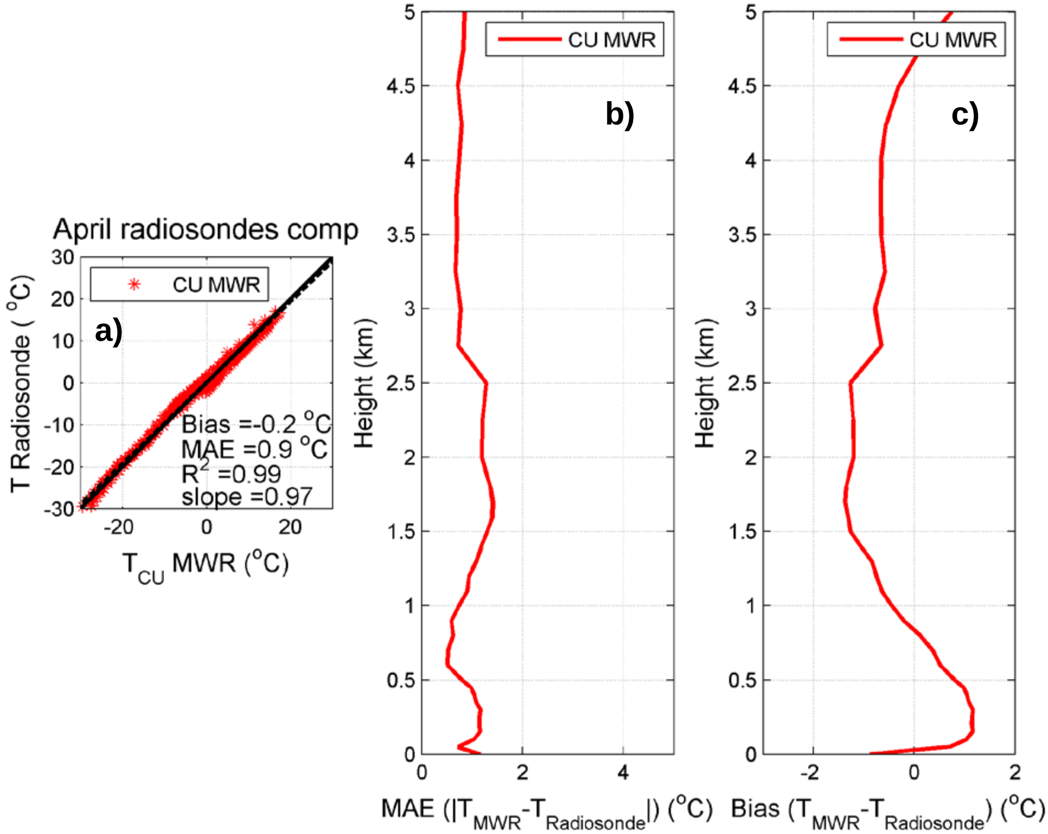

Figure 4: Same as in Fig. 3, but for 15 and 20 – 22 April including 10 radiosonde launches. Note that the pressure sensor of the NOAA MWR was broken between 5 – 27 April, therefore the NOAA MWR vs radiosonde comparison (*T*) over this period is not presented.

Atmos. Meas. Tech. Discuss., doi:10.5194/amt-2016-321, 2016
Manuscript under review for journal Atmos. Meas. Tech.
Published: 12 October 2016

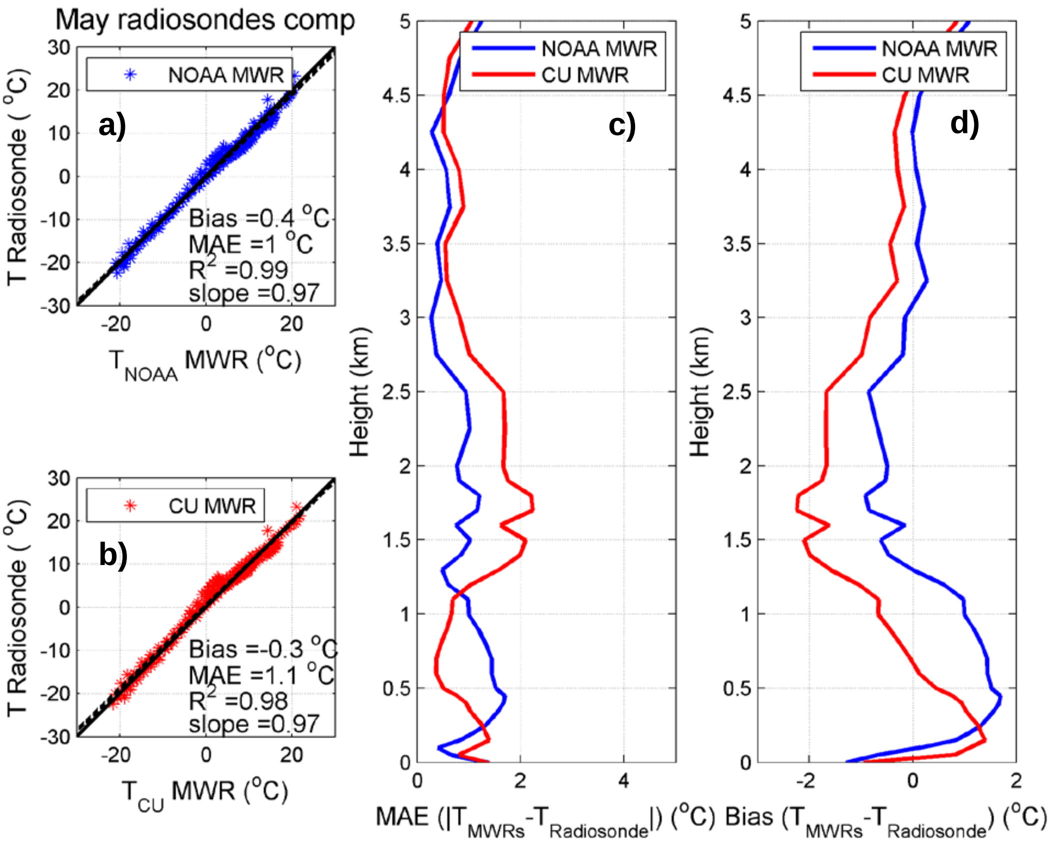

Figure 5: Same as in Fig. 3, but for the May period of 13 radiosonde launches.

Atmos. Meas. Tech. Discuss., doi:10.5194/amt-2016-321, 2016
Manuscript under review for journal Atmos. Meas. Tech.
Published: 12 October 2016

Atmospheric Measurement Techniques
Discussions

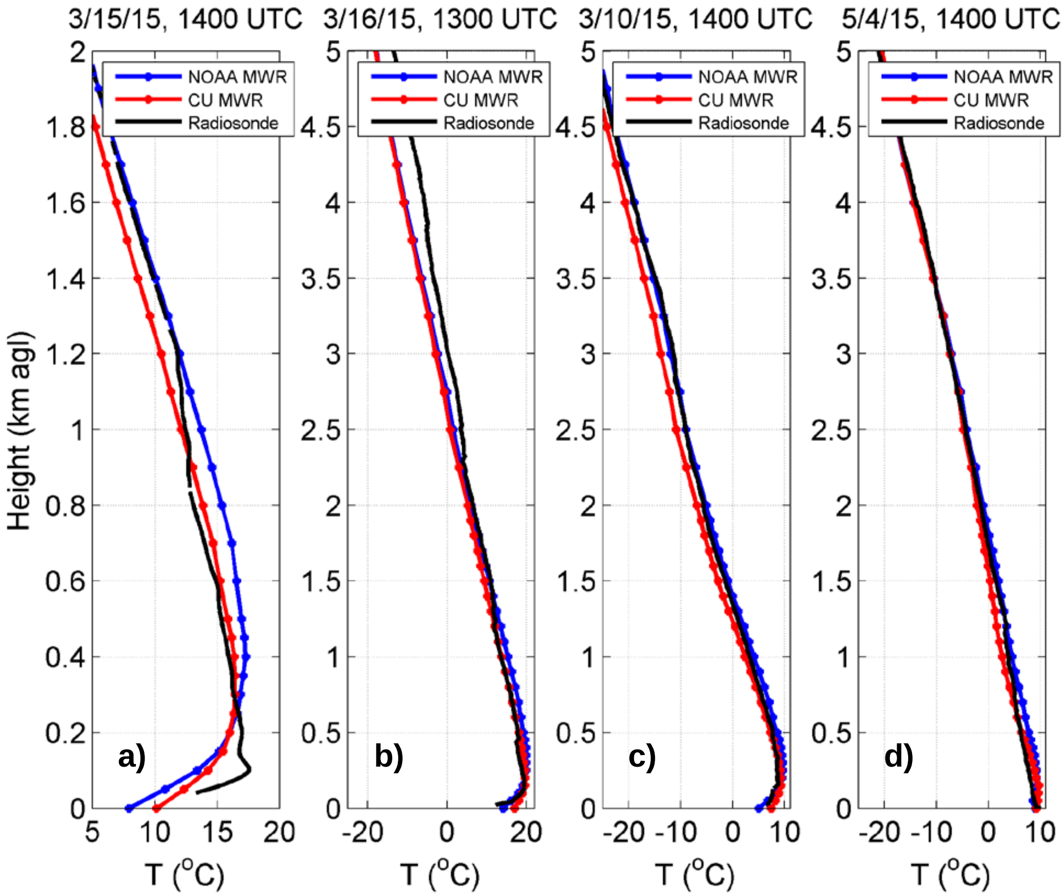

Figure 6: Vertical profiles of temperature as observed by MWRs (blue line: NOAA MWR; red line: CU MWR) and radiosonde (black line) at: a) 0800 LT (1400 UTC) on 15 March, b) 0700 LT (1300 UTC) on 16 March, and c) 0800 LT (1400 UTC) on 10 March 2015, d) 0800 LT (1400 UTC) on 4 May 2015.

Atmos. Meas. Tech. Discuss., doi:10.5194/amt-2016-321, 2016
Manuscript under review for journal Atmos. Meas. Tech.
Published: 12 October 2016

Atmospheric Measurement Techniques Discussions
Open Access
EGU

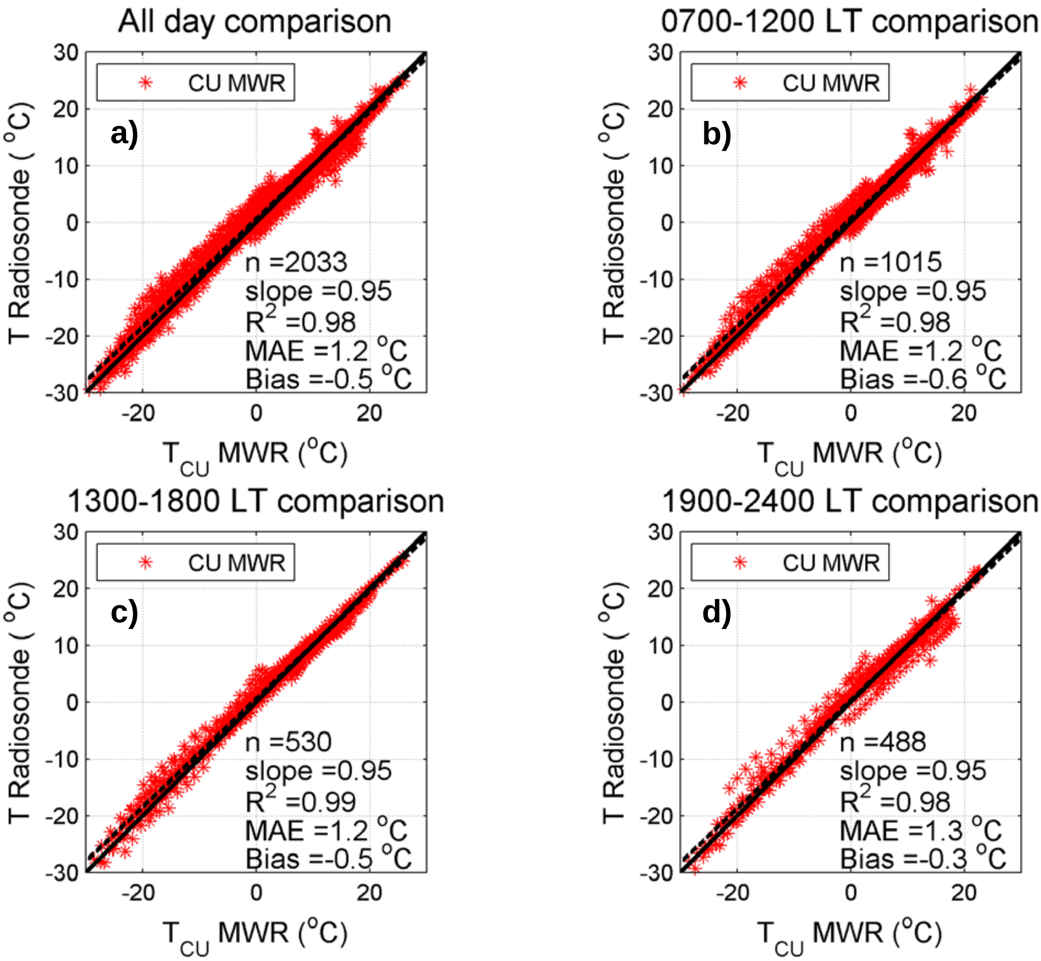

Figure 7: CU MWR vs radiosonde comparison of temperature over: a) 0700 – 2400 LT, b) 0700 – 1200 LT, c) 1300 – 1800 LT, and d) 1900 – 2400 LT between the surface and 5 km AGL. Data were collected on 9 – 19 March (38 soundings), 15 April and 20 – 22 April (10 soundings), and 1 – 4 May (13 soundings). Note that no radiosonde were launched between 0100-0600 LT. One-on-one line is indicated as solid black line and the regression as dashed black line.

Atmos. Meas. Tech. Discuss., doi:10.5194/amt-2016-321, 2016
Manuscript under review for journal Atmos. Meas. Tech.
Published: 12 October 2016

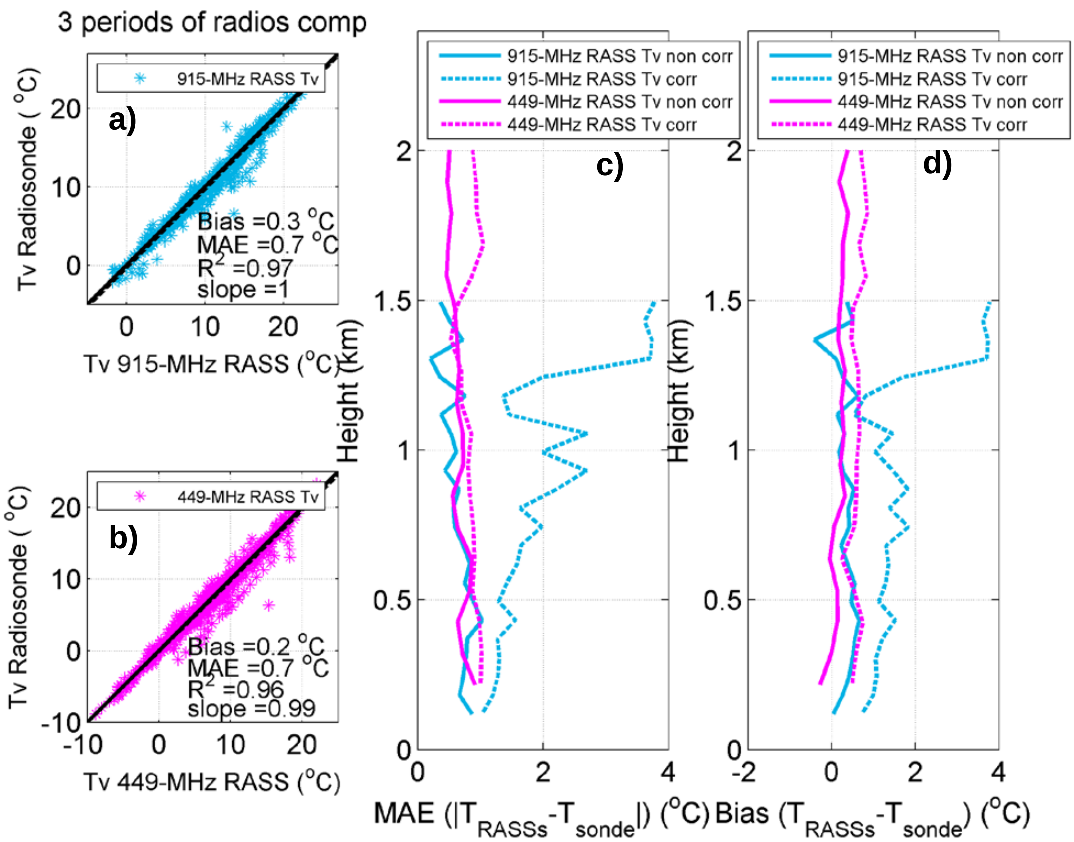

Figure 8: 915-MHz RASS (light blue) and 449-MHz RASS (magenta) vs radiosonde comparison of *Tv* over the 3 periods (March, April, and May) of radiosonde launches combined together. a)-b) One-to-one comparison between radiosonde and a) 915-MHz between 120 m and ~1.6 km AGL and b) 449-MHz RASS between 217 m – ~2 km AGL. The correction for the vertical velocity was NOT applied. One-on-one line is indicated as solid black line and the regression as dashed black line. c)-d) Vertical profiles of MAE and Bias for T_v with (dashed lines) and without (solid lines) vertical velocity correction.

Atmos. Meas. Tech. Discuss., doi:10.5194/amt-2016-321, 2016
Manuscript under review for journal Atmos. Meas. Tech.
Published: 12 October 2016

Atmospheric Measurement Techniques
Discussions

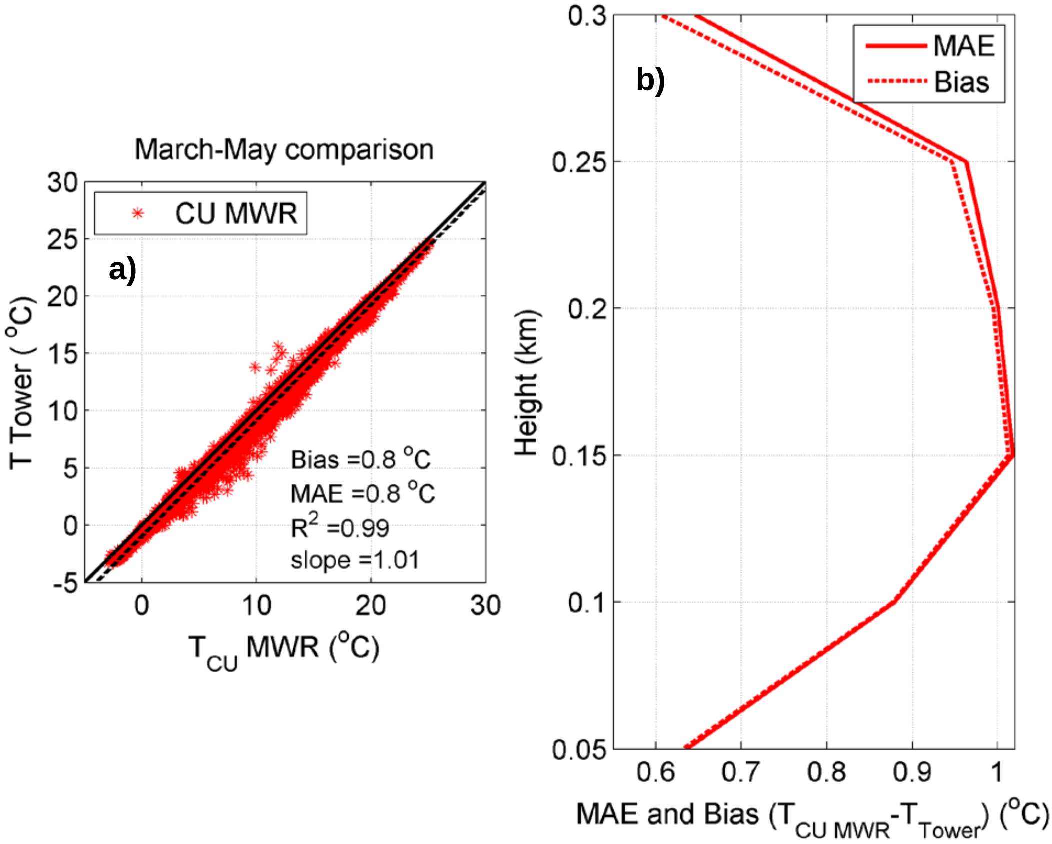

Figure 9: CU MWR vs tower comparison of temperature for all dates between 9 March – 7 May. a) One-to-one comparison. One-on-one line is indicated as solid black solid line and the regression as dashed black line. b) Vertical profiles of MAE and Bias for the same variable. Temperatures were observed at the tower at 50, 100, 150, 200, 250, and 300 m AGL, which collocates with MWR levels.

Atmos. Meas. Tech. Discuss., doi:10.5194/amt-2016-321, 2016
Manuscript under review for journal Atmos. Meas. Tech.
Published: 12 October 2016

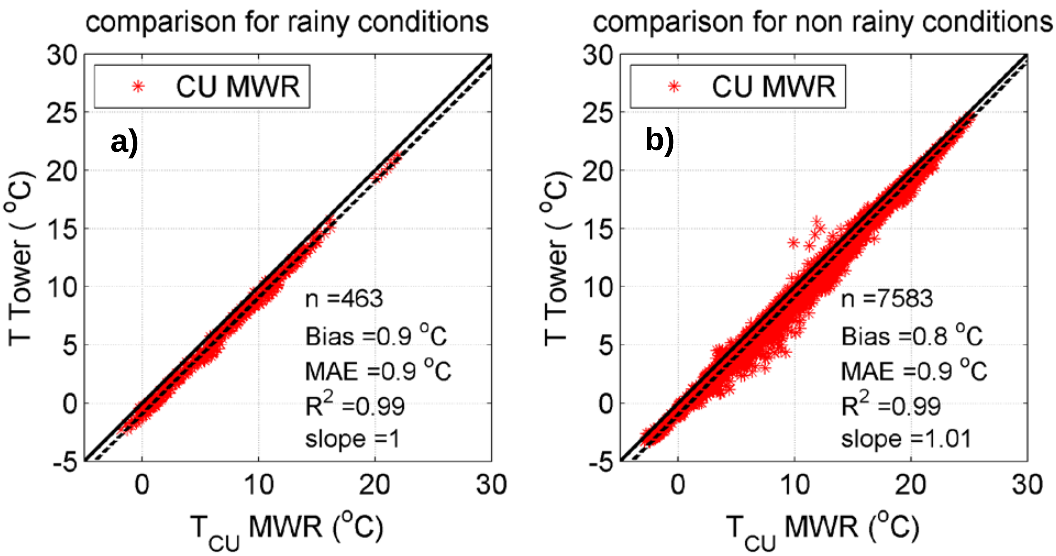

Figure 10: CU MWR vs tower temperature measurements during: a) rainy conditions, b) no-rain conditions as measured by the CU MWR. One-on-one line is indicated as black solid line and the regression as dashed black line.

Atmos. Meas. Tech. Discuss., doi:10.5194/amt-2016-321, 2016
Manuscript under review for journal Atmos. Meas. Tech.
Published: 12 October 2016

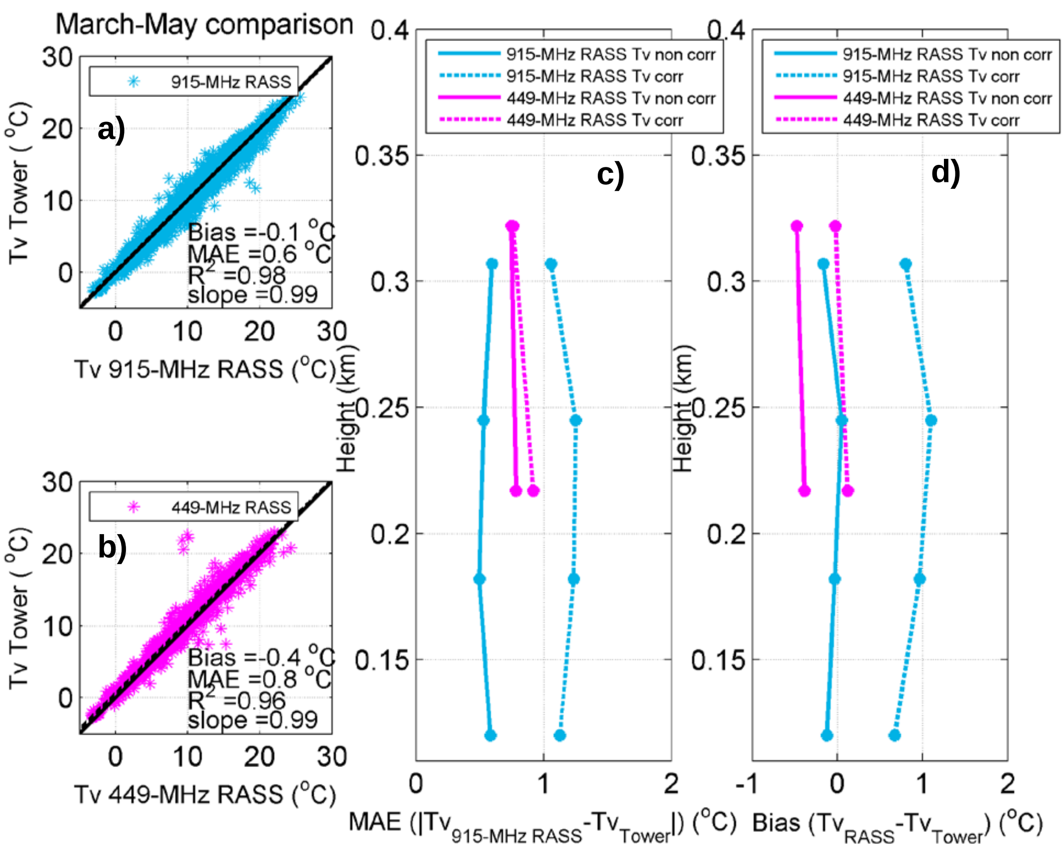

Figure 11: 915-MHz (light blue) and 449-MHz (magenta) RASS vs tower comparison of T_v for all dates between 9 March – 7 May. a-b) One-to-one comparisons between in-situ tower observations and uncorrected T_v observations. One-on-one line is indicated as solid black line and the regression as dashed black line. c)-d) Vertical profiles of MAE and Bias for T_v with (dashed lines) and without (solid lines) the vertical velocity correction. Height is AGL.

Atmos. Meas. Tech. Discuss., doi:10.5194/amt-2016-321, 2016
Manuscript under review for journal Atmos. Meas. Tech.
Published: 12 October 2016

Atmospheric Measurement Techniques
Discussions

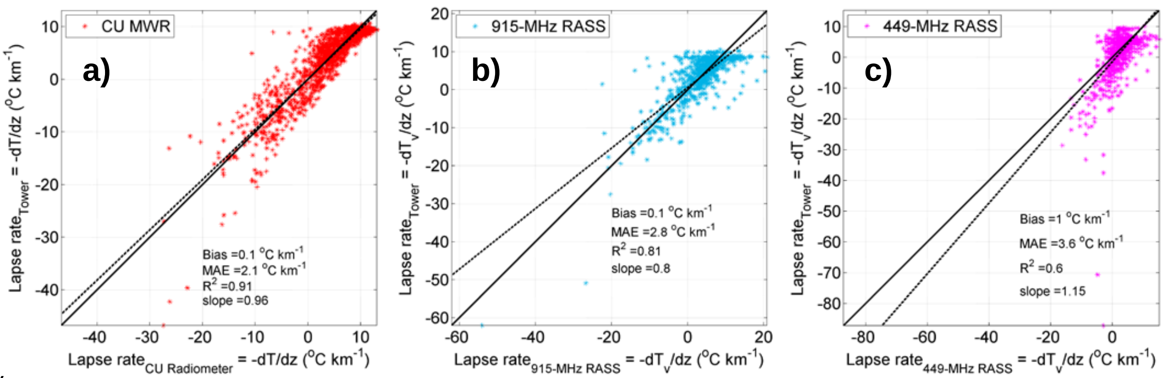

Figure 12: Comparison of atmospheric lapse rate for all dates between 9 March – 7 May, 2015 for: a) CU MWR vs tower (between first and last level of the tower measurements, 50-300m), b) 915-MHz RASS vs tower (between first and fourth level of the 915-MHz RASS measurements, 120-307m), c) 449-MHz RASS vs tower (between first and second level of the 915-MHz RASS measurements, 217-322m). Negative lapse rate represents stable atmospheric conditions. One-on-one line is indicated as solid black line and the regression as dashed black line.

Atmos. Meas. Tech. Discuss., doi:10.5194/amt-2016-321, 2016
Manuscript under review for journal Atmos. Meas. Tech.
Published: 12 October 2016

Atmospheric Measurement Techniques Discussions
Open Access

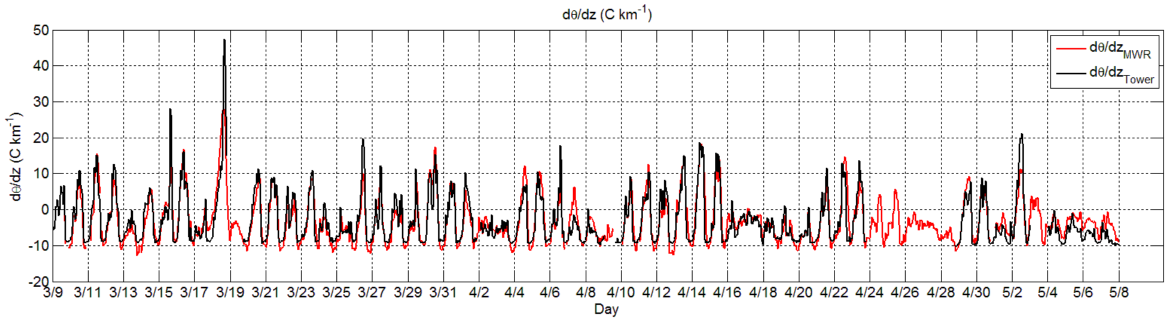

Figure 13: Lapse rate of potential temperature between 50 and 300 m AGL derived from observations conducted by the CU MWR (red line) and from tower observations (black line) for all dates between 9 March – 7 May.

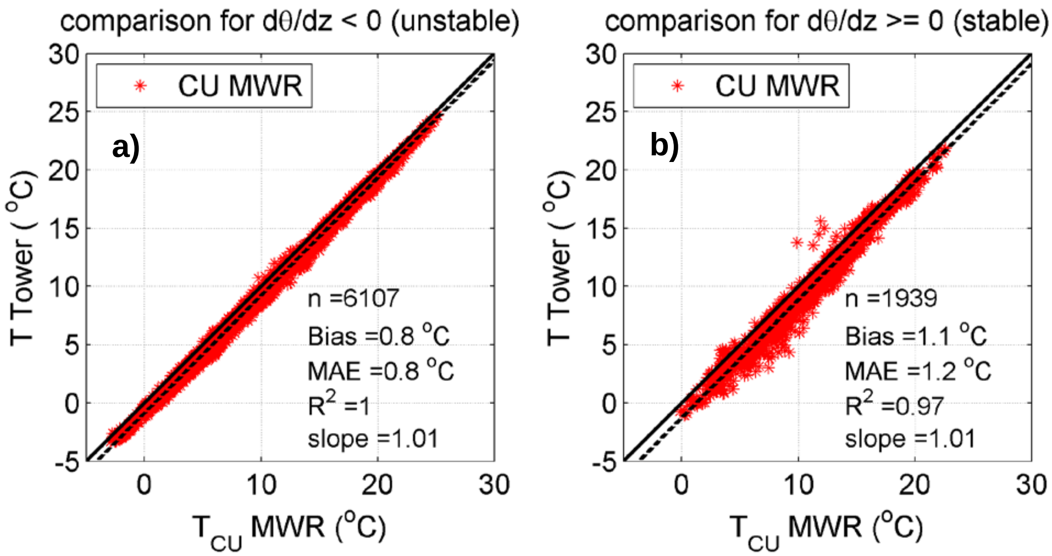

Figure 14: CU MWR vs tower comparison of T for all dates between 9 March – 7 May, for: a) $d\vartheta/dz < 0$, b) $d\vartheta/dz \geq 0$ between 50 – 300 m. Stability was determined by temperature differences measured by the CU MWR. One-on-one line is indicated as solid black line and the regression as dashed black line.

Atmos. Meas. Tech. Discuss., doi:10.5194/amt-2016-321, 2016
Manuscript under review for journal Atmos. Meas. Tech.
Published: 12 October 2016

Atmospheric Measurement Techniques Discussions

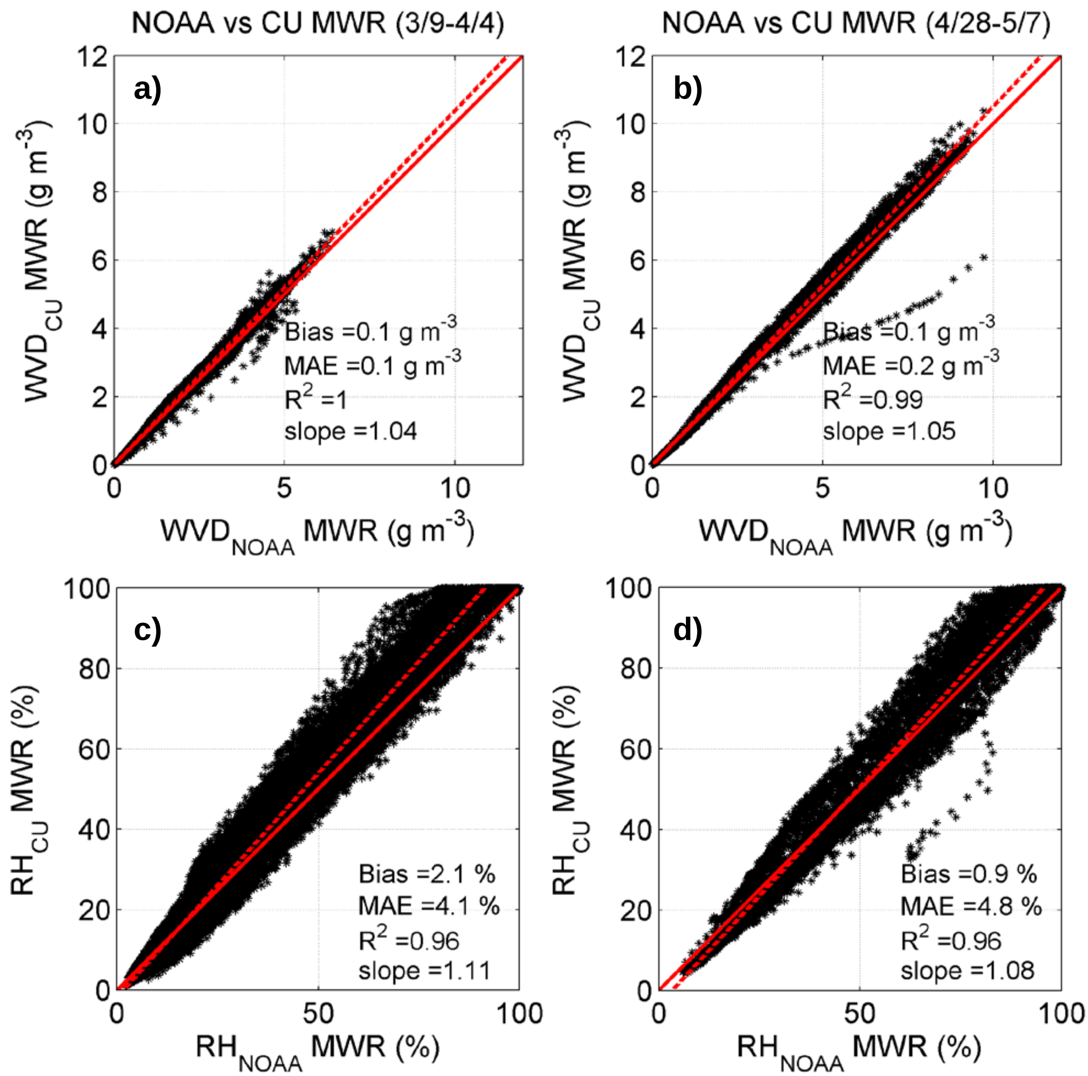

Figure 15: Comparison between a-b) *WVD* and c-d) *RH* observed by CU MWR and NOAA MWR between 9 March – 4 April 2015 (a and c) and 28 April – 7 May 2015 (b and d). The missing days in April coincide with the failure of the NOAA MWR surface sensor. One-on-one line is indicated as solid red line and the regression as dashed red line.

Atmos. Meas. Tech. Discuss., doi:10.5194/amt-2016-321, 2016
Manuscript under review for journal Atmos. Meas. Tech.
Published: 12 October 2016

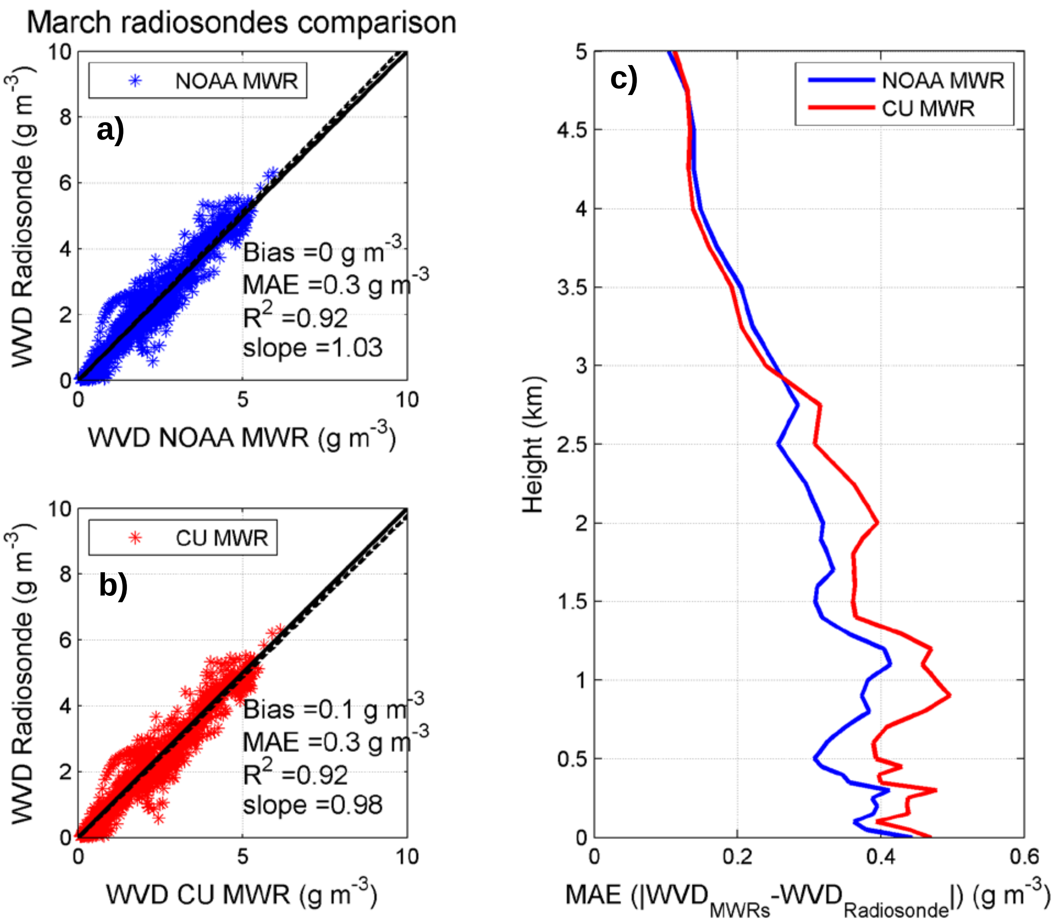

Figure 16: MWR vs radiosonde comparison of *WVD* over the March period of 38 radiosonde launches. a)-b) are one-to-one comparisons of *WVD* observed by the radiosondes and the a) NOAA and b) CU MWR between the surface and 5 km AGL. One-on-one line is indicated as solid black line and the regression as dashed black line. c) Vertical profiles of MAE for the same variable.

Atmos. Meas. Tech. Discuss., doi:10.5194/amt-2016-321, 2016
Manuscript under review for journal Atmos. Meas. Tech.
Published: 12 October 2016

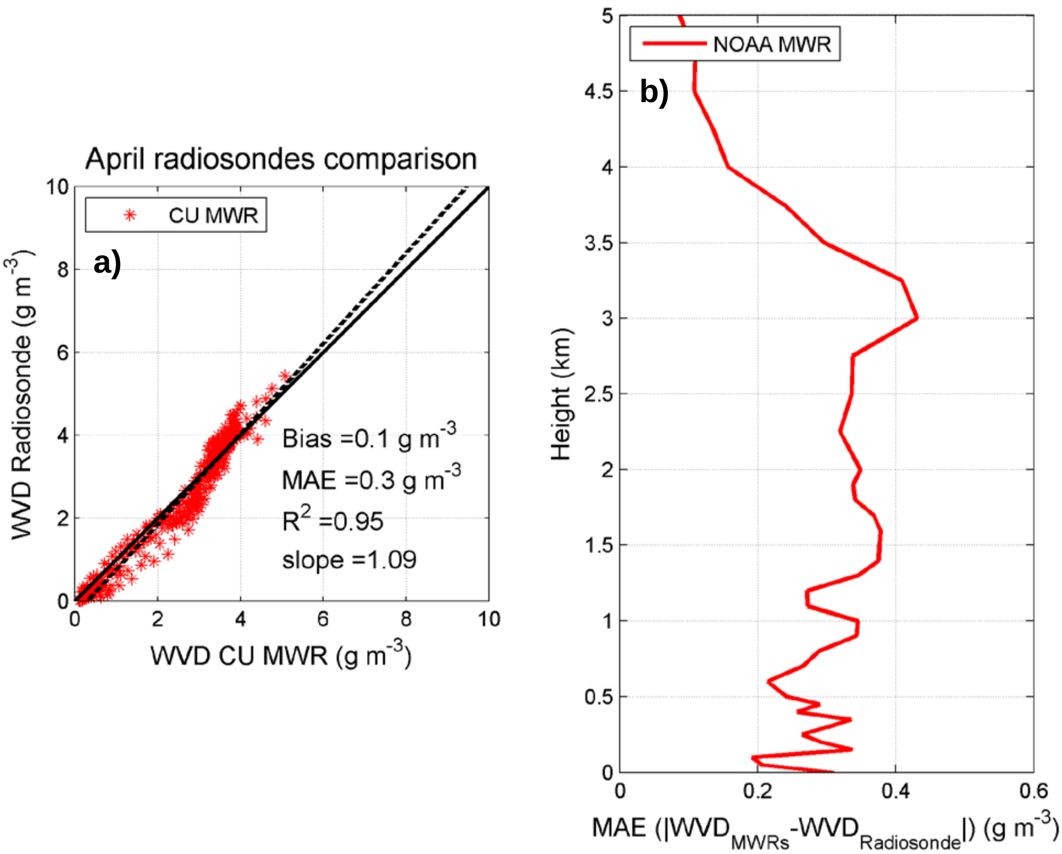

Figure 17: Same as in Fig. 16, but for 15 and 20 – 22 April including 10 radiosonde launches. Note that the pressure sensor of the NOAA MWR was broken between 5 – 27 April, therefore the NOAA MWR vs radiosonde comparison (*WVD*) over this period is not presented.

Atmos. Meas. Tech. Discuss., doi:10.5194/amt-2016-321, 2016
Manuscript under review for journal Atmos. Meas. Tech.
Published: 12 October 2016

Atmospheric Measurement Techniques Discussions

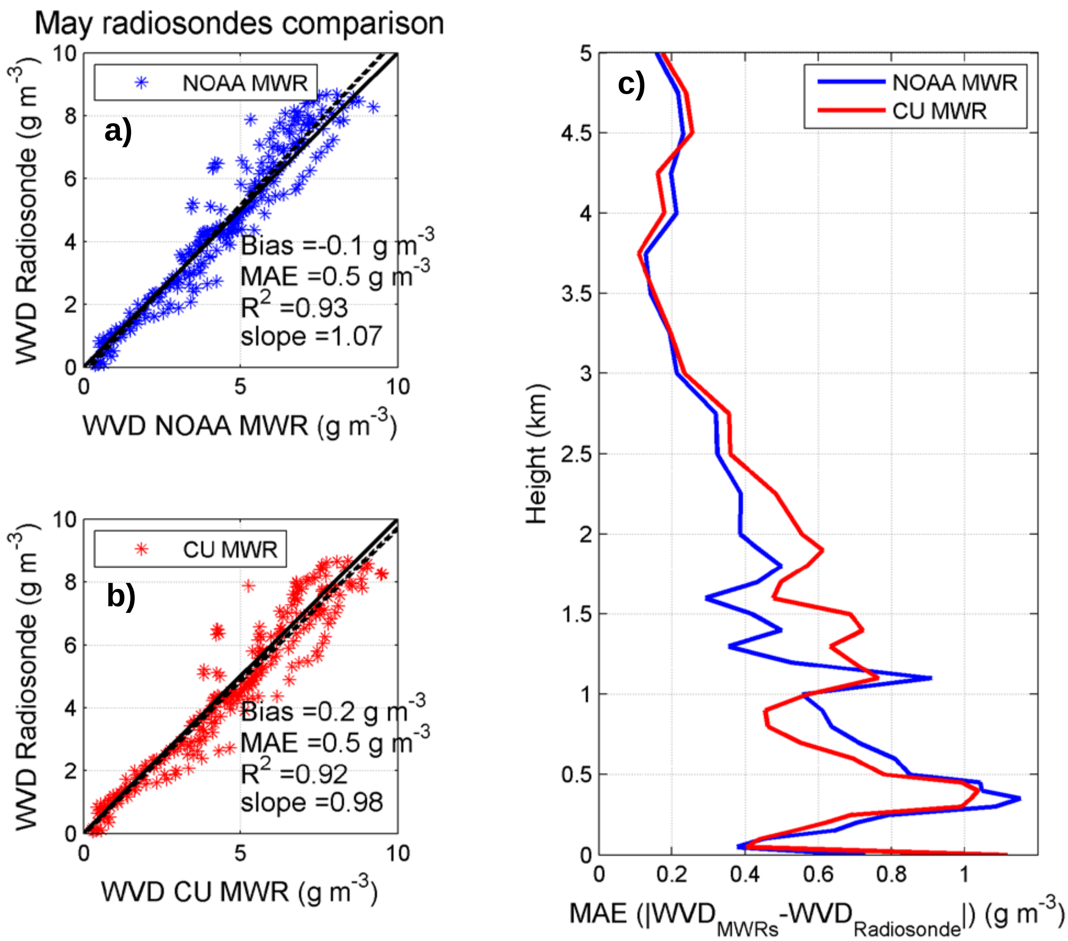

Figure 18: Same as in Fig. 16, but for the May period of 13 radiosonde launches.

Atmos. Meas. Tech. Discuss., doi:10.5194/amt-2016-321, 2016
Manuscript under review for journal Atmos. Meas. Tech.
Published: 12 October 2016

Atmospheric Measurement Techniques
Discussions

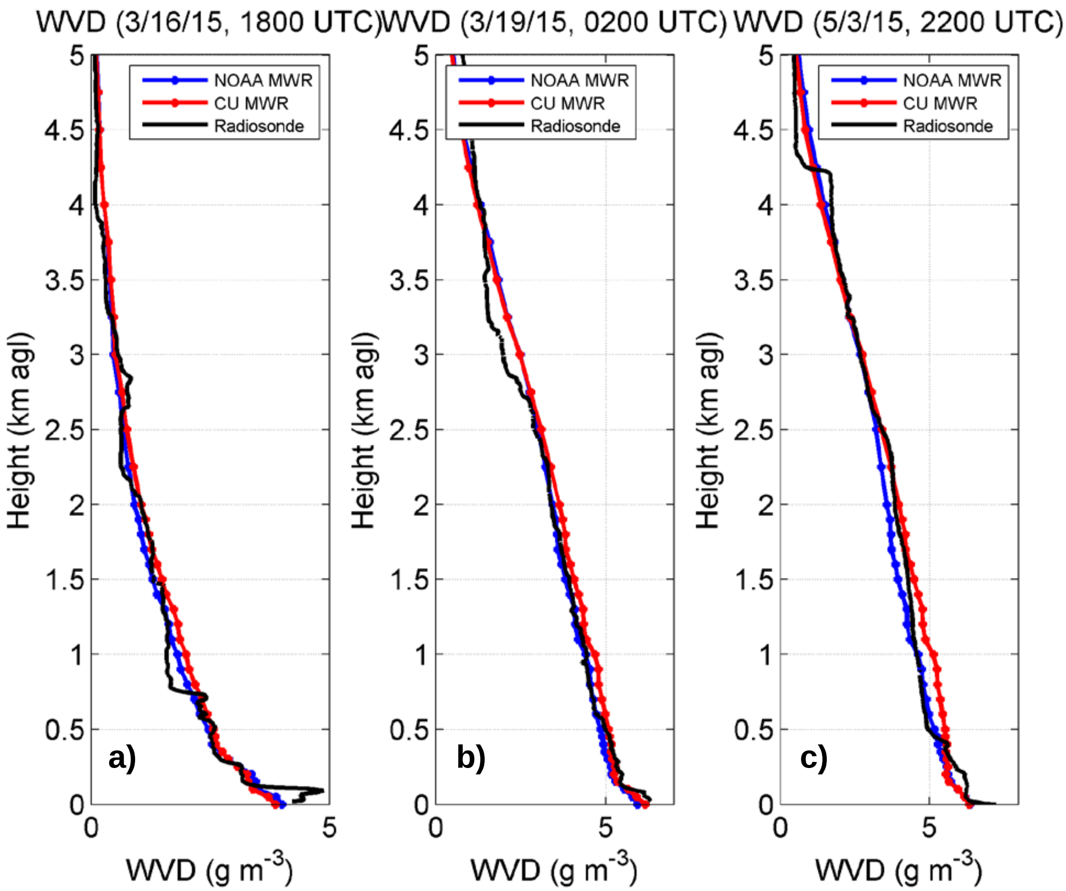

Figure 19: Vertical profiles of *WVD* as observed by MWRs (blue line: NOAA MWR; red line: CU MWR) and radiosonde (black line) at a) 1800 LT (0000 UTC) on 16 March, b) 0200 LT (0800 UTC) on 19 March, and c) 2200 LT (0400 UTC) on 3 May 2015.

Atmos. Meas. Tech. Discuss., doi:10.5194/amt-2016-321, 2016
Manuscript under review for journal Atmos. Meas. Tech.
Published: 12 October 2016

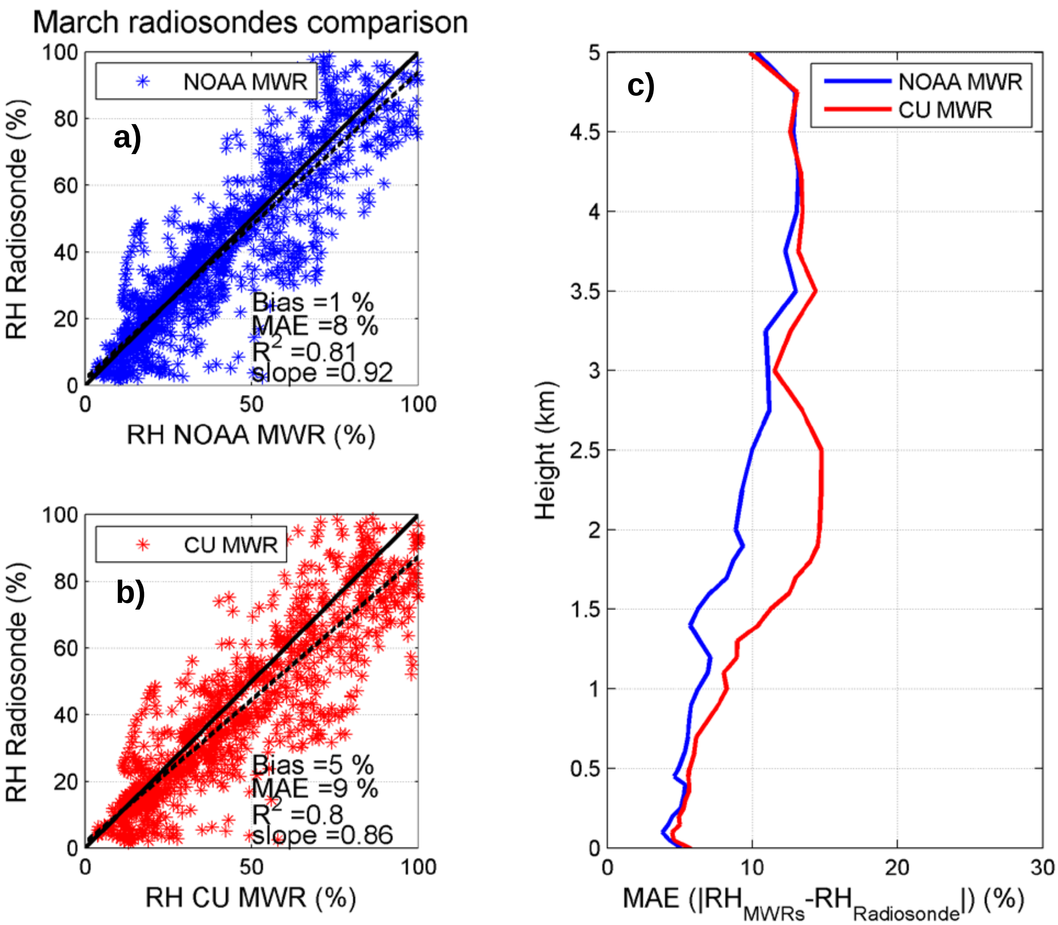

Figure 20: MWR vs radiosonde comparison of *RH* over the March period of 38 radiosonde launches. a)-b) are one-to-one comparisons of *RH* observed by the radiosondes and the a) NOAA and b) CU MWR between the surface and 5 km AGL. One-on-one line is indicated as solid black line and the regression as dashed black line. c) Vertical profiles of MAE for the same variable.

Atmos. Meas. Tech. Discuss., doi:10.5194/amt-2016-321, 2016
Manuscript under review for journal Atmos. Meas. Tech.
Published: 12 October 2016

Atmospheric Measurement Techniques
Discussions

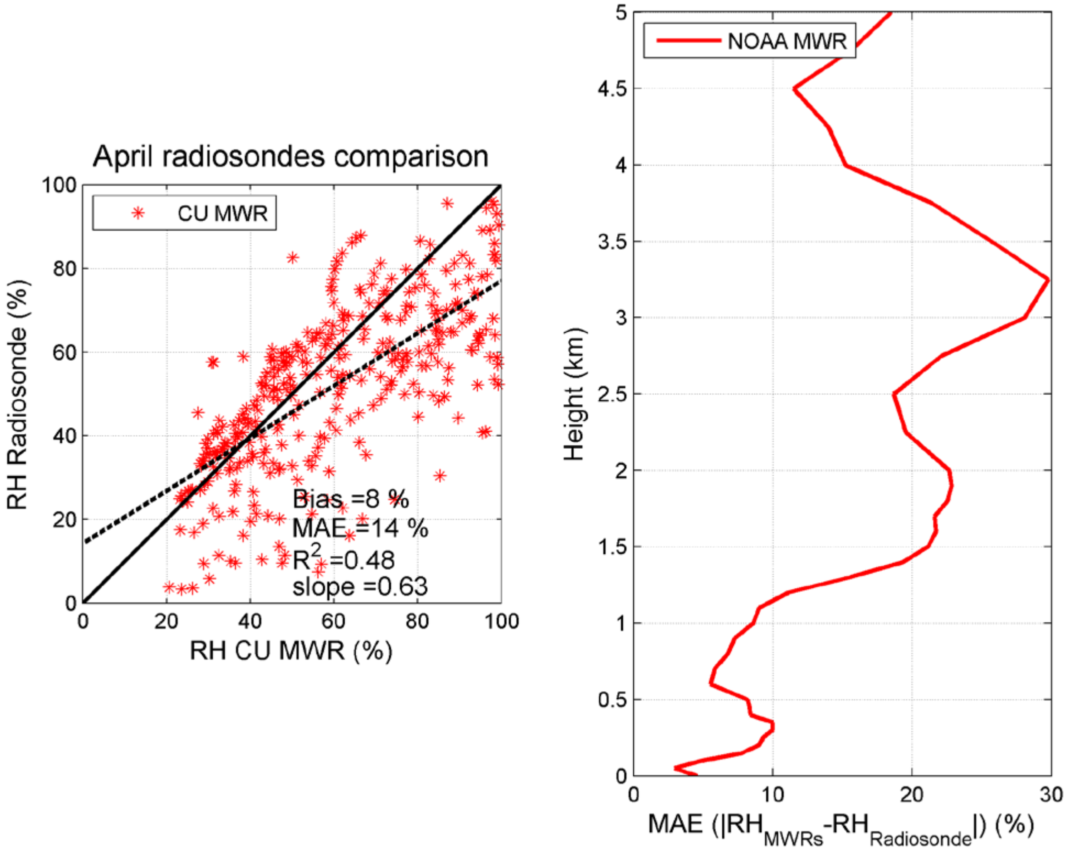

Figure 21: Same as in Fig. 20, but for 15 and 20 – 22 April including 10 radiosonde launches. Note that the pressure sensor of the NOAA MWR was broken between 5 – 27 April, therefore the NOAA MWR vs radiosonde comparison (*RH*) over this period is not presented.

Atmos. Meas. Tech. Discuss., doi:10.5194/amt-2016-321, 2016
Manuscript under review for journal Atmos. Meas. Tech.
Published: 12 October 2016

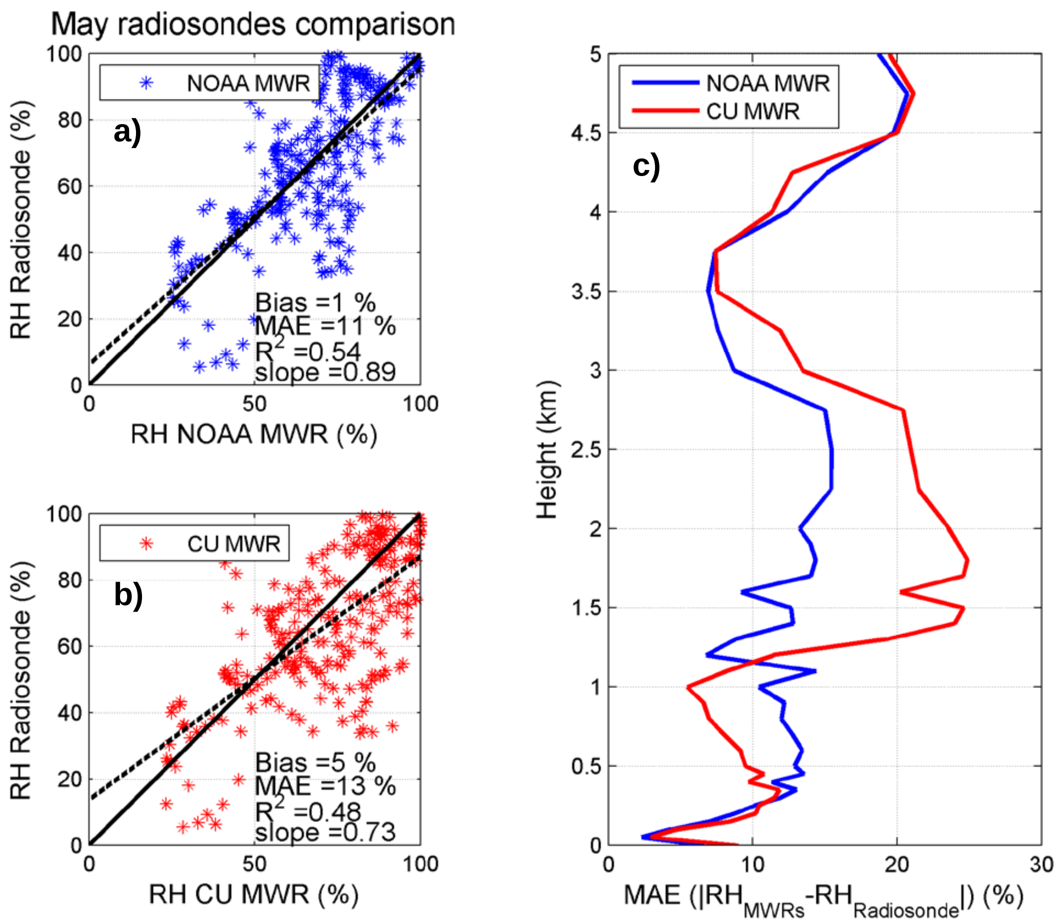

Figure 22: Same as in Fig. 20, but for the May period of 13 radiosonde launches.

Atmos. Meas. Tech. Discuss., doi:10.5194/amt-2016-321, 2016
Manuscript under review for journal Atmos. Meas. Tech.
Published: 12 October 2016

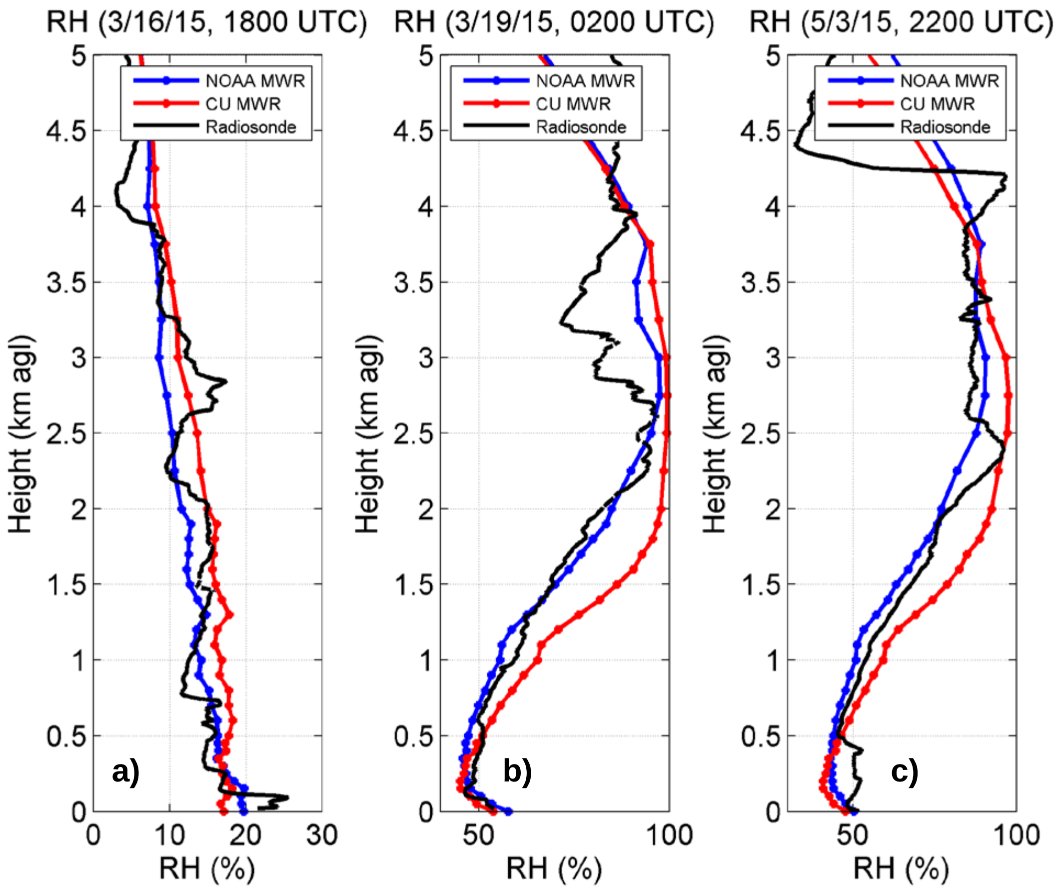

Figure 23: Vertical profiles of *RH* as observed by MWRs (blue line: NOAA MWR; red line: CU MWR) and radiosonde (black line) at a) 1800 LT (0000 UTC) on 16 March, b) 0200 LT (0800 UTC) on 19 March, and c) 2200 LT (0400 UTC) on 3 May 2015.